

EXPERIMENTS WITH A STRATOSPHERIC GENERAL CIRCULATION MODEL

I. RADIATIVE AND DYNAMIC ASPECTS

SYUKURO MANABE and BARRIE G. HUNT¹

Geophysical Fluid Dynamics Laboratory, ESSA, Washington, D.C.

ABSTRACT

An 18-vertical level primitive equation general circulation model was developed from previous models of the Geophysical Fluid Dynamics Laboratory in order to study the lower stratosphere in detail. The altitude range covered was from the surface to 4 mb. (37.5 km.), the vertical resolution being optimized in the tropopause region to permit a more accurate calculation of the vertical transport terms. A polar stereographic projection was used and the model was limited to a single hemisphere.

The model now resolves two distinct jet streams, one in the troposphere and the other in the middle polar stratosphere. The wind systems produce a 3-cell meridional structure in the troposphere, which evolves into a 2-cell structure in the stratosphere. However, the wind structure and associated features of the model in the troposphere had a general equatorward shift compared with observation.

A considerable improvement was also obtained in some features of the temperature distribution, in particular the local midlatitude temperature maximum in the lower stratosphere is well defined and shown to be dynamically maintained. The low temperature and sharpness of the equatorial tropopause temperature distribution are closely reproduced by the model, and these features are attributed to the action of the upwards branch of the direct meridional cell in the Tropics, as is the basic cause of the difference in height of the tropopause at low and high latitudes.

The energy balance of the lower stratosphere in the present model agrees better with observation than previous models did, and confirms earlier work that this region is maintained from the troposphere by a vertical flux of energy. A similar flux of energy is also required to maintain the middle stratosphere, even though this region generates kinetic energy internally, and it is concluded that it is only marginally possible that this region may be baroclinically unstable. It appears that forcing from below extends to higher altitudes in winter than previously suspected.

CONTENTS

Abstract.....	477
1. Introduction.....	477
2. Description of the model.....	479
3. Initial conditions and time integration.....	479
4. State of quasi-equilibrium.....	480
4.1. Zonal mean temperature.....	480
4.2. Mean flow field.....	482
5. Angular momentum balance of the atmosphere.....	485
6. Heat balance of the atmosphere.....	486
6.1. Latitude-height distribution of heat balance components.....	487
6.2. Variation of the vertical temperature profile with latitude.....	489
6.2.1. Tropics.....	489
6.2.2. High latitudes.....	490
6.2.3. Tropopause gap.....	491
6.2.4. Tropopause height variation.....	491
6.3. Temperature distribution in the stratosphere.....	492
7. Maintenance of the winter stratosphere.....	494
7.1. Wind distribution in the stratosphere.....	494
7.2. Energy balance of the middle and lower stratosphere.....	496
7.3. Some comments on the baroclinic nature of the stratosphere.....	498
8. Concluding remarks.....	501
References.....	501

1. INTRODUCTION

General circulation models present a unique theoretical tool for studying the large-scale behavior of the atmosphere, and, since the first model was introduced by Phillips [34], they have provided considerable insight into the processes responsible for the maintenance of the observed state of the atmosphere. Following Phillips, Smagorinsky [36] presented a detailed study based on his application of the primitive equations to general circulation models, and at the present time, comprehensive, multilevel models have been developed by Smagorinsky, Manabe, and Holloway [37]; Manabe, Smagorinsky, and Strickler [19]; Mintz [22] and Leith [14]; Kasahara and Washington [9]; and Kurihara and Holloway [13]. These models were mainly concerned with meteorological aspects of the general circulation, although their potentialities for use in simulating other roles of the atmosphere such as transport studies have been illustrated by the inclusion of the hydrologic cycle in the work of Manabe et al. [19].

¹ Attached to GFDL under an Australian Public Service Scholarship. Now returned to Weapons Research Establishment, South Australia.

Most of the above mentioned general circulation models were primarily designed to represent the behavior of the troposphere. Following their success in this regard, and, although much remains to be done in simulating the troposphere, it is a logical development to extend the models upwards in order to study the stratosphere in more detail than was possible previously. To date relatively little effort has been expended on modeling the stratosphere, the most comprehensive work being that of Smagorinsky et al. [37] and Manabe et al. [19] whose general circulation models had the top two or three layers in the lower stratosphere. Although they had rather coarse vertical resolution in the stratosphere, the former partially explained a long-standing question concerning how the latitudinal temperature distribution in the lower stratosphere is maintained. The question posed was why does the lower stratosphere have a temperature maximum in middle latitudes and a minimum temperature at the Equator? They were able to show that the dynamics of the atmosphere played an important role in this temperature structure and, in particular, that the subtropics were cooled by large-scale eddies transporting heat counter-gradient, in agreement with the observations of White [43]. Smagorinsky et al. also discussed the energy balance of the stratosphere, and found that the model was in approximate agreement with observation, part of the discrepancy being attributed to poor resolution of the vertical transport of geopotential from the troposphere. Insufficient vertical resolution was also considered to be responsible for the inadequate reproduction of the thermal structure around the tropopause. Manabe et al. successfully simulated the observed dryness of the stratosphere in their study, and thus provided some much-needed insight into this controversial matter. The only other modeling study of the stratosphere appears to be that of Peng [33], who used a truncated spectral model, together with the geostrophic approximation, to study specifically the energy balance and the temperature gradient of the lower stratosphere. He obtained results which corresponded fairly well with the more complete general circulation studies, and the thermal structure of his model atmosphere was actually in closer agreement with the atmosphere. This may have been due to the manner in which the static stability was specified in his model, or to the other approximations involved in his approach.

The present model was planned with two objectives in view. The first of these was to investigate the diffusion of tracer material in the stratosphere, since this has never been done previously with a general circulation model. As might be imagined, there is considerable interest in understanding how the radioactive debris resulting from nuclear tests in the atmosphere is transported and precipitated, and also how the distribution of a minor constituent such as ozone is maintained, in view of its importance to the radiative properties of the atmosphere. The second objective was to study the energy balance and heat balance of the lower stratosphere in more detail

than was possible previously, by using a model with better resolution for the representation of the vertical energy flux. The effect of the vertical resolution of the model was somewhat unknown, and, apart from expecting an improvement in the stratosphere, it was not obvious whether a similar improvement might be obtained in the troposphere. The question as to what is the ideal vertical resolution for a numerical study of the atmosphere is not easily answered without doing empirical calculations.

The two objectives of this study were not quite compatible as regards their requirements for vertical resolution, and the ultimate choice was a compromise, considerations of computation time making it necessary to keep the number of levels to a minimum. The model which eventually resulted was an 18-vertical level model developed from the 9-level model of Smagorinsky et al. [37], who will hereafter be referred to as *S*. The 9-level model covered the altitude range 0–31.6 km., and was designed to resolve the atmospheric boundary layer in some detail with the resolution coarsening at the upper levels, while the 18-level model extended from 0–37.5 km. and had a fairly uniform resolution with respect to geometrical height, but no attempt was made to resolve the Ekman boundary layer. The altitude of the top model level was determined by the minimum pressure at which it was considered that the radiation calculation in the model could be carried out accurately. The method by which radiative transfer was computed in the model was essentially that described by Manabe and Strickler [20].

The increase in the model's vertical resolution produced rather remarkable improvements in some aspects of the model's similarity to the atmosphere, and also revealed some new features compared with the previous 9-level model. As a result it was decided to discuss the dynamical part of this model in more detail than originally planned; consequently Part I of this paper is solely concerned with meteorological aspects, while Part II (Hunt and Manabe [7]) will be concerned with the diffusion of tracers in the atmosphere as represented by the model. However, it is not the intention to give as detailed a discussion of the results as was given by *S* for their 9-level model. The emphasis here will be partially to contrast the present results with their results in order to illustrate the differences produced by the higher vertical resolution, although the heat balance of the stratosphere will be analyzed in some depth as this seems to be justified.

It should be pointed out that there appears to be a flaw in the model which to date has evaded discovery. Several features of minor importance in the 9-level model have been greatly accentuated in the present model, presumably because of the increased vertical resolution. The most damaging of these is the generation of a small reverse cell in the tropical troposphere, and the manner in which the model maintains its angular momentum balance, which is now different from that of the atmosphere. Despite this flaw it is thought that the analysis and results to be presented are of general validity.

2. DESCRIPTION OF THE MODEL

The model used in this experiment was essentially that described by *S*, apart from some minor changes resulting from the conversion of the 9 levels in that model to the 18 levels required for the tracer study. The system of equations and their finite difference formulation, and the details of the model will therefore not be repeated here, and only a brief, qualitative description emphasizing the modifications made will be given.

The model consisted of a hemispheric, polar stereographic projection with a nonconducting, free-slip "wall" at the Equator. Neither mountains nor land-sea contrast were included, and no explicit allowance was made for condensation of water vapor in the atmosphere, i.e., the model was "dry." The moist convective adjustment procedure described in the previous paper was, however, incorporated in order to obtain a realistic static stability. Also the same radiative transfer scheme was used, except for more recent data for the ozone and water vapor distributions. The ozone profiles were based on the distributions published by Hering and Borden [6], which were obtained from measurements over North America with chemi-luminescent sondes. Their seasonal distributions were combined to give a mean value for the year, and the data so obtained were normalized to make them agree with the total ozone amounts given by London [17], as London's values were based on a longer, worldwide series of measurements. In the case of water vapor, only the stratospheric distribution was changed to make it correspond with the "dry" observations of Mastenbrook [21] and Williamson and Houghton [44], a mass mixing ratio of 3×10^{-6} being assumed. The radiative calculations were carried out for a mean zenith angle which was

constant with time, a corresponding mean value of the solar radiation input being used; in this way the day-night contrast was removed from the model.

Horizontal diffusion was incorporated exactly as in the previous paper but, because the vertical resolution of the 18-level model did not resolve the boundary layer, a different procedure had to be devised for the vertical diffusion. Since the closest level to the earth's surface was situated at a height of 0.85 km. (see fig. 1) it was assumed that it was representative of the free atmosphere, and the wind velocity at the anemometer level (circa 6 m.) was extrapolated from the wind velocity of this level. The anemometer velocity was taken to be 0.6 of that of the free atmosphere and to lag it by 20° , these values being based on the work of Rossby and Montgomery [35]. No allowance was made for the variation of these factors with latitude. The anemometer velocity was then used to calculate the upward flux of momentum and the upward flux of sensible heat at the earth's surface, using the same expressions as given previously by *S*. Because of the depth of the layer adjacent to the surface in the 18-level model, the momentum and heat fluxes transferred from the earth's surface were assumed to be completely assimilated in this layer only. In the 9-level model this approximate treatment was, of course, unnecessary.

The computational space mesh required for representing the finite difference analog of the governing equations corresponded to an $N=20$ system, i.e., there were 20 grid points between the Pole and the Equator, giving approximately 1,200 points per level. The primitive equations were used for the equations of motion and a normalized pressure $Q=p/p_*$ (p_* , surface pressure) was chosen as the vertical coordinate. The levels of vertical finite differencing are defined by the following analytic function:

$$Q_k = \frac{B}{A} [\exp(A\sigma_k) - 1]$$

where $A=3.24$, $B=0.132$, and $\sigma_k = \frac{2k-1}{36}$, ($k=1, 2, 3, \dots, 18$).

Definition of the vertical levels by a simple analytic function prevents an irregular change of layer thickness with altitude, and thus helps to reduce the truncation error involved in the vertical derivatives.

The details of the Q coordinate system are given in table 1 and figure 1. These values were arrived at by computing Q at the half levels, obtaining ΔQ_k as the difference between the half level values, and then defining Q_k as the difference between $Q_{k+1/2}$ and $\frac{1}{2}\Delta Q_k$. This procedure was used to ensure the conservation properties of total energy for the finite difference scheme (see Kurihara and Holloway [13]).

3. INITIAL CONDITIONS AND TIME INTEGRATION

The general circulation study reported by *S* had as its initial condition an isothermal atmosphere at rest, and they found that it required approximately 200 days to reach a state of thermal equilibrium. Since the results are

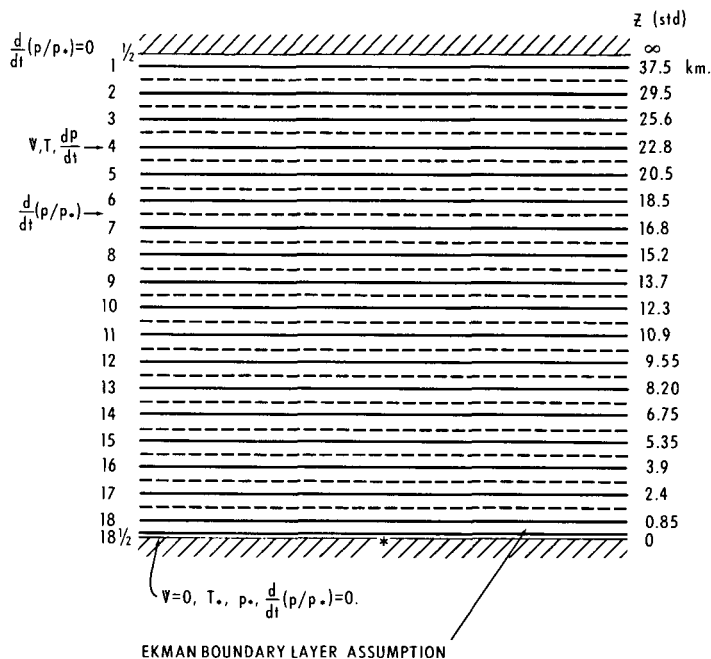


FIGURE 1.—The Q levels used in the model and their approximate heights. The levels at which the model variables are predicted are indicated.

TABLE 1.—*Q levels used in the model*

Level	σ	Q	Q at half level
1	1/36	0.0040	0.0080
2	3/36	0.0129	0.0177
3	5/36	0.0234	0.0292
4	7/36	0.0361	0.0430
5	9/36	0.0512	0.0595
6	11/36	0.0694	0.0793
7	13/36	0.0911	0.1029
8	15/36	0.1171	0.1313
9	17/36	0.1482	0.1652
10	19/36	0.1855	0.2058
11	21/36	0.2301	0.2545
12	23/36	0.2836	0.3127
13	25/36	0.3475	0.3824
14	27/36	0.4241	0.4658
15	29/36	0.5158	0.5657
16	31/36	0.6256	0.6854
17	33/36	0.7570	0.8286
18	35/36	0.9143	1.0000

analyzed for the period when the model is in a quasi-steady state, it is desirable to reduce the initial transient state to as short a time as possible. For this reason the present study was not started from rest, but from the time-averaged zonal mean values of the zonal wind U , surface pressure p^* , and temperature distribution T obtained by extrapolating and interpolating the data from the analysis period of the 9-level model of S to the 18 levels of the present model. It was hoped that the transients produced by this data manipulation would be damped out rapidly, and that the model would reach its quasi-steady state much faster than in the previous study.

Unfortunately this ideal was not quite achieved because the initial conditions based on the zonally averaged data, together with the interpolation and extrapolation used, produced an imbalance in the dynamic state of the model. This resulted in the excitation of a planetary inertia-gravity wave of period approximately 11.5 hr. In addition to this inertia-gravity wave the initial conditions produced a large, transient rise in the hemispheric mean kinetic energy of the model, as indicated in figure 2, which reached a peak at 12 days. This transient rise corresponded to the transition from the axis-symmetric flow regime to the wave regime. The figure also shows the inertia-gravity wave and how it damped out over a period of about 55 days. Despite the production of this disturbance it is thought that equilibrium was still attained faster than would have been if an isothermal atmosphere at rest had been used as the initial condition.

The development of baroclinic waves was triggered in the model after 5 days by applying a random perturbation within the range $\pm 0.1^\circ\text{C.}$ to the temperature field. The model appeared to reach a quasi-steady state at about 85 days, at which time the tracer distributions discussed in Part II [7] were initiated. Some development subsequently took place after this time, notably in the stratosphere, as the response time of the model was particularly slow for this region. The model was run for a total of 265 days, the external forcing of the model via the solar radiation input being kept constant throughout this period so that a state of quasi-equilibrium was maintained.

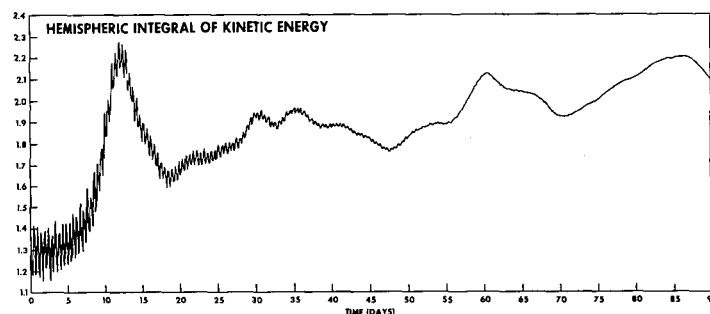


FIGURE 2.—Time variation of the hemispheric integral of kinetic energy illustrating the instability produced by the initial conditions and its subsequent damping. (Units: 10^2 joule.)

4. STATE OF QUASI-EQUILIBRIUM

The results presented in this and subsequent sections, unless otherwise stated, were derived by analyzing data at 6-hr. intervals, and time averaging over the last 100 days of the experiment. The distributions of the basic meteorological variables will be given here in order to provide an overall idea of how the model compared with the actual atmosphere, before discussing what dynamic and radiative processes were involved in the maintenance of the computed state. In comparing the model with observation it should be recalled that, in reality, there is no annual mean atmosphere. In spite of the use of annual mean insolation values the model appears in some ways to be representative of late autumn and early winter conditions in the atmosphere, although somewhat different results might be expected if the model had made a seasonal march in order to reach this time of year.

As regards the observational side of the atmosphere, a point of some consequence is that land-sea contrast and orography influence such properties of the atmosphere as the position of the jet stream and the height of the tropopause. When a zonal mean value of these terms is derived a smoothing out of the perturbations produced by these effects occurs, and this could, for example, result in a zonal mean maximum value which was less than the maximum value of any individual meridional cross section. In the model this particular source of perturbations is missing, and there is a somewhat more uniform variation of properties with longitude, and this tends to produce zonal means which are more representative of extreme values. A further point is that very few meaningful, zonally averaged results are available above about 25 km. in the atmosphere, and the observed results given here for the upper levels were therefore derived from a variety of rather heterogeneous sources, and they may not be very representative of the real atmospheric situation.

4.1. ZONAL MEAN TEMPERATURE

In figure 3, a comparison is given of the latitude height distribution of the zonal mean temperatures for the observed winter and annual mean conditions, together with those computed by the 9- and 18-level models.

The data below 50 mb. were abstracted from the results of Starr's group which are based on 5 yr. of observations. At higher levels results were taken from Oort [31], Batten

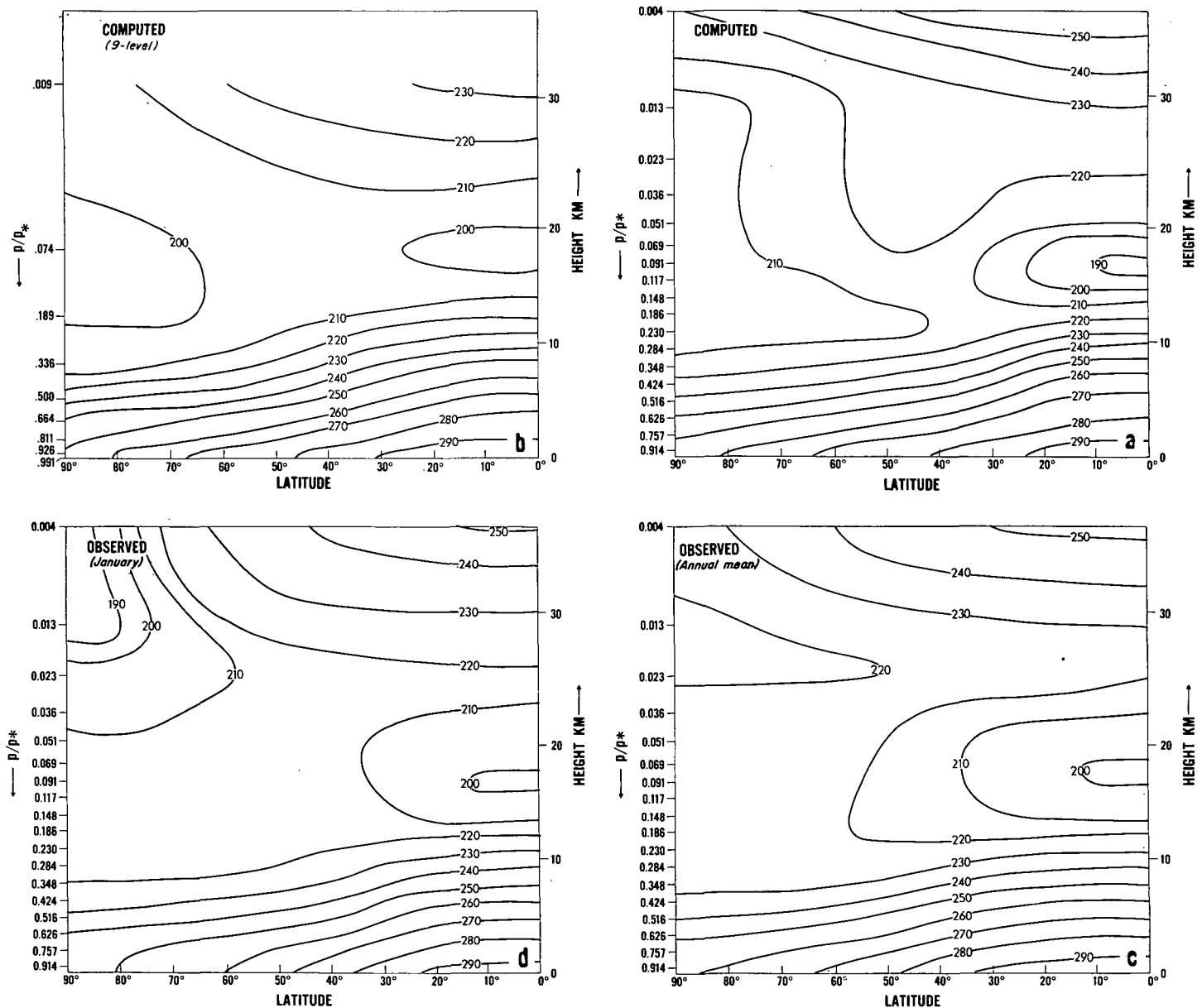


FIGURE 3.—The latitude-height distribution of the zonal mean temperature. In the upper half of the figure the temperatures computed by the 18- and 9-level models are shown on the right and left respectively. In the lower half observed temperatures for annual mean and January conditions are given for comparison, based largely on the results of Starr and collaborators. (Units: °K.)

[2], the Handbook of Geophysics [45], and Muench and Borden [25]. Overall both models simulate the atmospheric temperature structure rather well, although there are a number of differences in the details, with the better agreement being with the annual mean values. The present model does not resolve the polar inversion in the lower troposphere because of the poor vertical resolution in the boundary layer. However, the Pole to Equator surface temperature difference of 42°C. is the same as that for the previous model and is in good agreement with the real annual average value. The latitudinal temperature gradient in the upper troposphere at middle latitudes is slightly smaller than previously, although it is still larger than in the atmosphere, resulting in too strong a jet stream.

The most outstanding improvement in the present model is in the horizontal temperature gradient in the

lower stratosphere, where a significant maximum is now achieved in middle latitudes. From the Equator to the maximum temperature at 45° latitude there is a rise of 29°C. at level 7 (91 mb.), while the Equator to Pole rise was 19°C. For the 9-level model these differences were only 14° and 5°C. respectively, the improvement being attributed to the more accurate calculation of the vertical heat flux, because of the higher vertical resolution, rather than to any improvement in the radiative calculations. This particular latitudinal temperature gradient is not a feature of the 5-yr. annual mean results, and only a monotonic temperature rise of 22°C. from the Equator to the Pole is observed. The reason for this appears to be connected with the rather high equatorial tropopause temperature obtained by Starr's group. Better agreement is obtained for an individual longitude, and a comparison of the latitudinal temperature gradient in the lower

stratosphere is presented in figure 4 for the 18-level model and for various times of the year based on Kochanski's [11] data. The model results are fairly close to the annual mean temperatures, except that the model maximum occurs about 15° latitude too far south. The observed annual mean Equator to maximum and Equator to Pole temperature differences are 27°C. and 22°C. respectively, which are quite close to those of the model, and it is the simulation of both these values which is of importance rather than the exact correspondence of the temperature distributions. It therefore appears that the model now simulates quite well one of the more difficult features of the atmosphere.

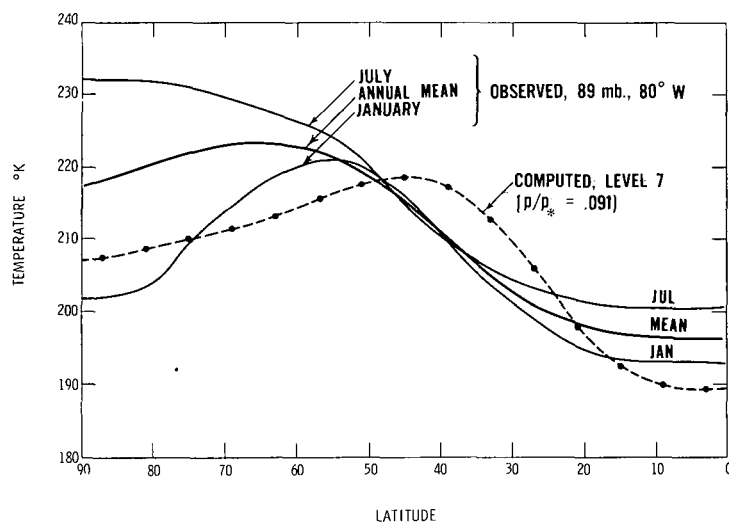


FIGURE 4.—The computed latitudinal variation of the temperature distribution in the lower stratosphere is compared with observations of Kochanski [11] at 80°W. for various times of the year.

In the top layer of the model (4 mb.) the Pole to Equator temperature rise is 28°C., which is close to the probable annual mean difference of about 30°C. The model temperatures do not agree very well with those in the middle polar stratosphere in the winter, but this is to be expected, because the model has insolation at these latitudes unlike the atmosphere at this time of year. This insolation is most important for the higher levels of the model, and throughout the middle stratosphere the model is warmer than the winter atmosphere.

In figure 5 temperature profiles for selected latitudes are compared with zonally averaged annual mean profiles of Starr's group, and these illustrate the quite satisfactory agreement attained. The model tropical tropopause is somewhat colder than observation, as mentioned previously, but apart from this both the 3° and 39° latitudinal profiles have similar lapse rates and temperature discontinuities as the atmosphere. In the lower polar stratosphere the model is about 10°C. colder than annual mean conditions, but the tropopause height is in good agreement with observation. The temperature structure around the tropopause is much more clearly resolved in the 18-level model than the previous model.

4.2. MEAN FLOW FIELD

In figure 6 the computed zonal wind for zonally averaged conditions is compared with the results for the 9-level model, and for annual mean conditions based on the analyses of Starr's group, Oort [31] and Batten [2]. In addition the January wind distribution given by Kochanski [11] for 80°W. is included. It is apparent that a notable improvement over the previous model has been obtained in some features of the wind distribution, in particular

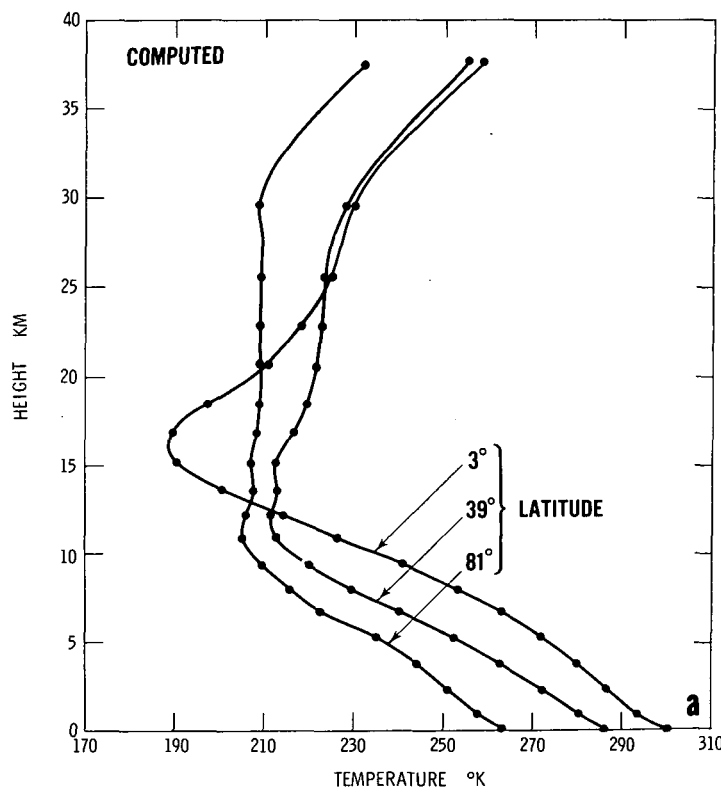
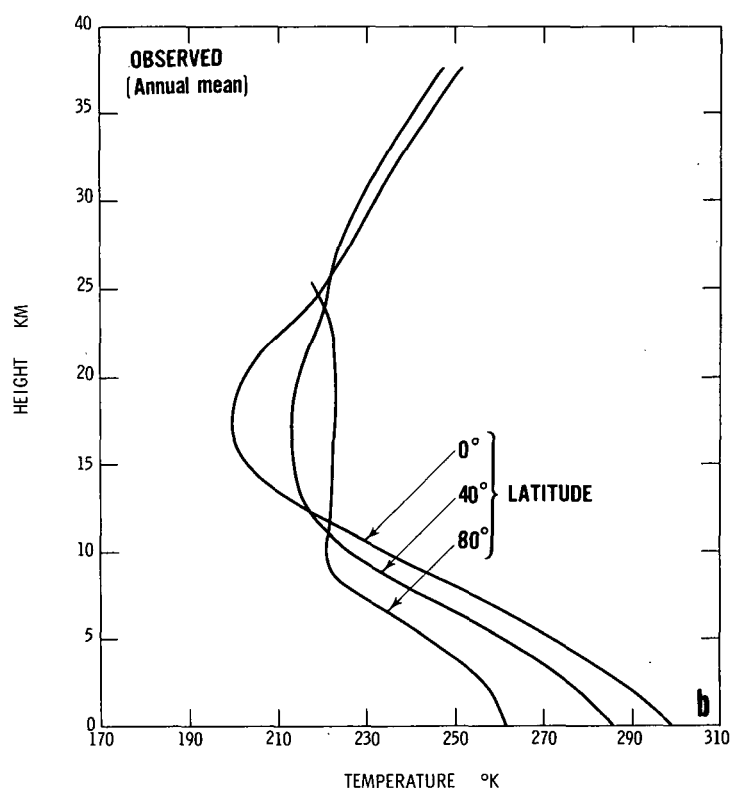


FIGURE 5.—The observed annual mean temperature profiles of Starr and collaborators for three different latitudes are compared with corresponding computed profiles.

both jet streams are now clearly resolved. Nevertheless, there is still room for considerable improvement in the present model, since compared with annual mean conditions the model tropospheric jet stream at 27° latitude is too far south by about 10° , and is also too intense by a factor of two. In this respect it might be noted that in the Southern Hemisphere according to Obasi [29] the jet stream is closer to the Equator, at about 30°S ., and this may reflect the shift of the thermal Equator into the Northern Hemisphere produced by the asymmetry of the topography between the hemispheres. The upper level jet stream is also too strong and slightly too far north, but the observational data are rather limited for a detailed comparison. The tropical easterlies in the middle stratosphere are better resolved than previously, although they are not quite strong enough and are not continuous to the surface. The surface easterlies at high latitudes extend too far south, and are worse than the 9-level model in this respect.

As observed by *S*, annual mean conditions perhaps should not be compared with the model because of the seasonal variation included in the atmosphere's annual mean distribution. The results of Kochanski [11] have therefore been included to show that, although the model

jet streams are rather strong, they are not unrepresentative of conditions which occur in the atmosphere from time to time. The observed westerly intensities for January are very similar to those of the model, and, while the model jet streams are both displaced to the south, the tilt of the jet stream axis is close to that depicted by Kochanski. The upper level jet stream, which is similar to the polar night jet, is noticeably higher than that observed at 80°W ., but it is interesting to note that the model produced such a distinct jet, despite insolation being present at high latitudes.

Even though the model appears to agree better with winter conditions as far as the zonal velocities are concerned, an inspection of the 5-yr. data analyzed by Starr's group shows that the zonal mean maximum intensity of the tropospheric jet for January averaged over this period was 35 m./sec. Possibly this was somewhat low because of smoothing associated with longitudinal perturbations of the jet stream, but there is no doubt that the model produces a rather strong jet stream, and an effort to find out the cause of this is currently underway.

The zonally averaged meridional and vertical velocities of the model are given in figure 7, together with the meridional velocities derived by Mintz and Lang [23]

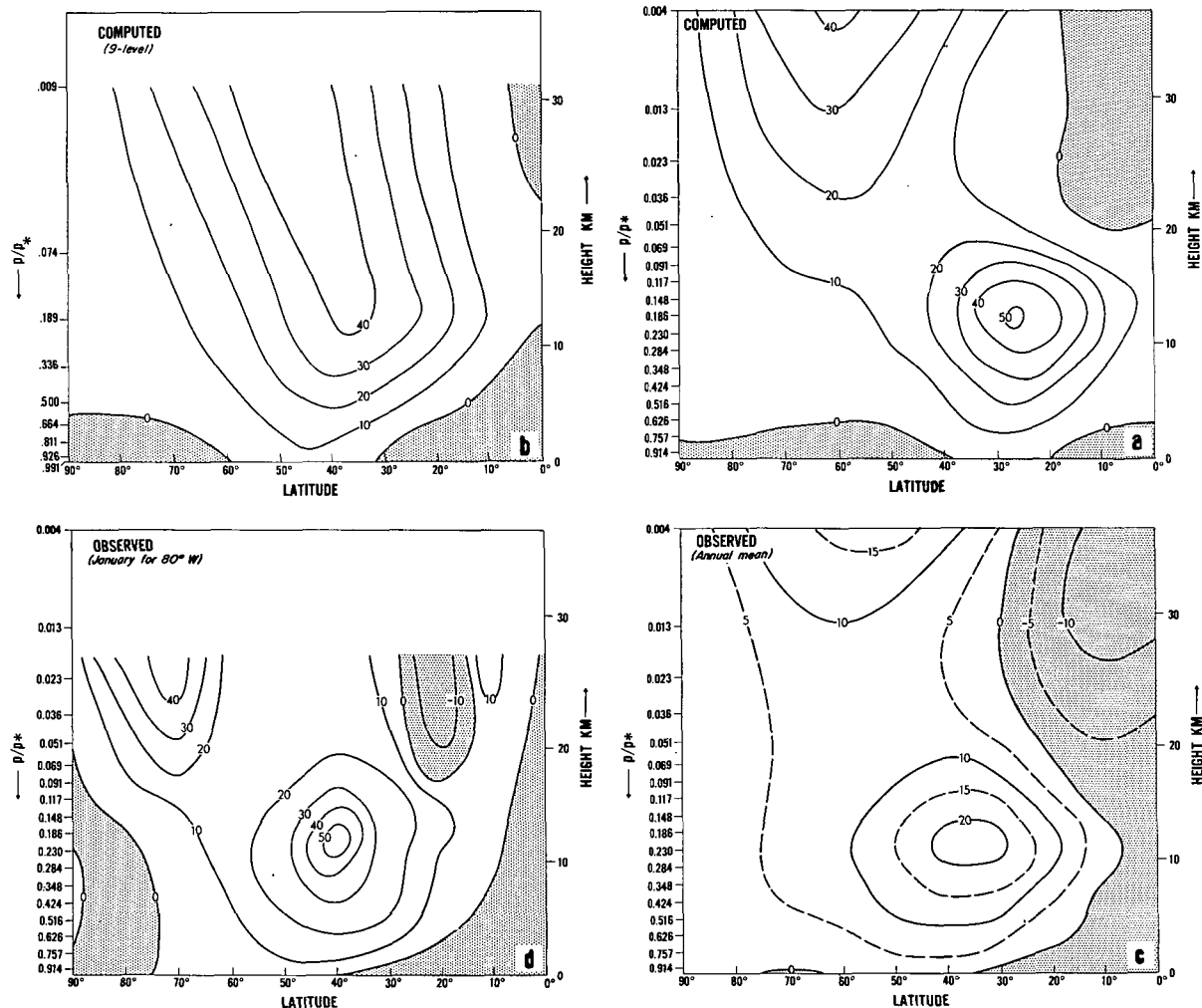


FIGURE 6.—The latitude-height distribution of the zonal mean zonal wind. In the upper half of the figure winds computed by the 18- and 9-level models are shown on the right and left respectively. In the lower half observed annual mean winds (principally Starr and collaborators) and also winds at 80°W . for January (Kochanski [11]) are given for comparison. Shaded areas are regions of easterly winds. (Units: m./sec.)

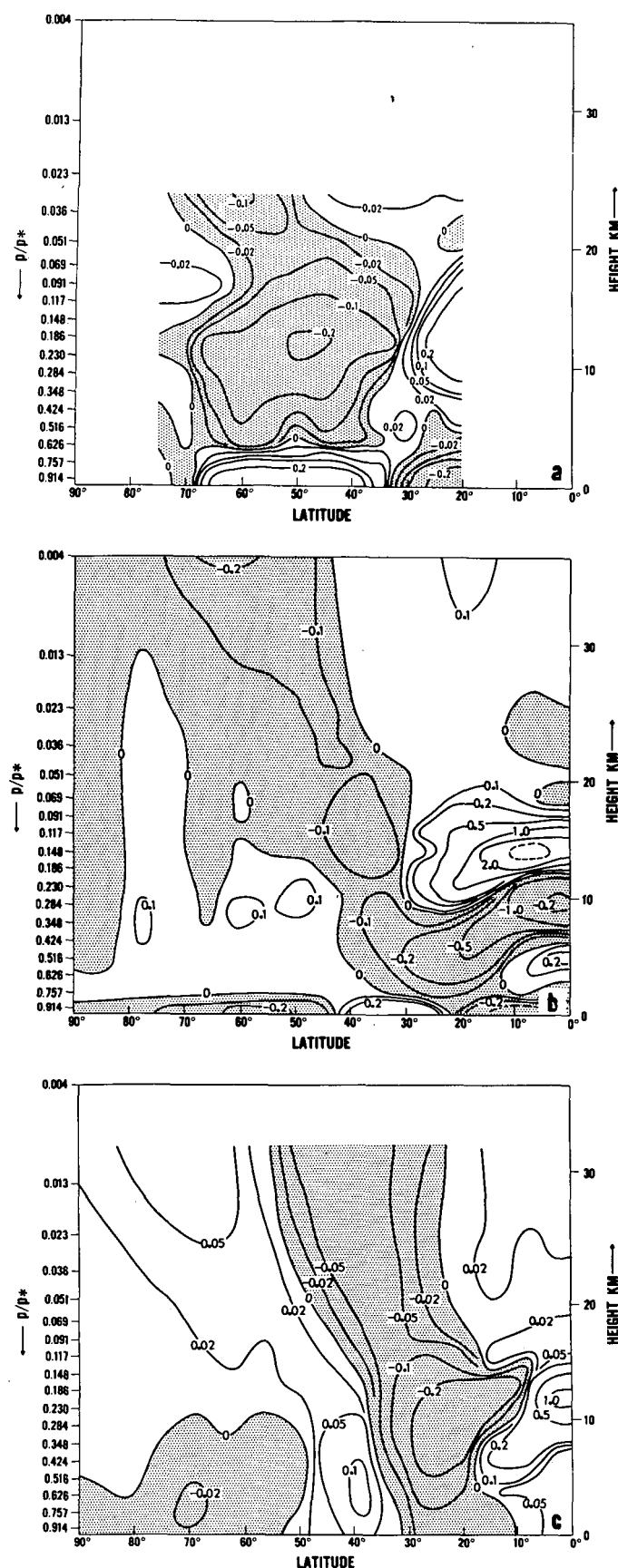


FIGURE 7.—The upper part of the figure shows the latitude-height distribution of the meridional wind component (m./sec.) obtained from the requirement of the angular momentum balance of the actual atmosphere. In the middle and lower parts are shown respectively the computed meridional component (m./sec.) and the corresponding vertical component of the wind (cm./sec.). Shaded areas are regions of downwards or equatorwards flow.

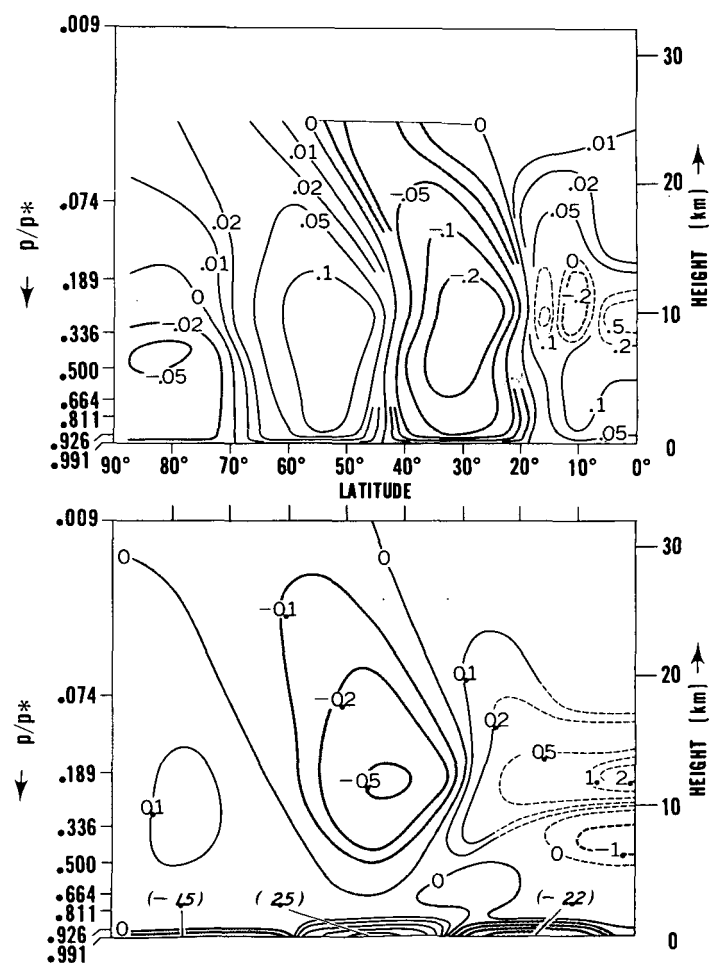


FIGURE 8.—The latitude-height distributions of the zonal means for the 9-level model of the computed vertical component of the wind (cm./sec.) and the corresponding meridional component (m./sec.) are given in the upper and lower parts of the figure respectively. Shaded areas are regions of downwards or equatorwards flow.

and Teweles [40] based on the budget of the angular momentum. In figure 8 the corresponding velocities for the 9-level model are also included for comparison. These figures reveal an unrealistic feature of the present model which was not so apparent in the earlier studies, this being the existence of quite strong (~ 1 m./sec.) northerly winds at about 10 km. at the Equator. These winds were sufficiently intense to penetrate to the subtropics where they joined up with the northerly winds which normally exist there. These northerly winds in the upper tropical troposphere are part of a reverse meridional cell which the model generates in this region and, although present previously, the higher vertical resolution of the current model may have accentuated this feature with the result shown in figure 7. The reason for the existence of this cell is unknown, but it is thought to be in some way connected with the "wall" at the Equator as it does not occur in another model developed at this Laboratory in which the wall has been removed. The higher resolution produced two regions of maximum northerlies in midlatitudes in agreement with observation, one in the lower, the other in the middle stratosphere ²

² For convenience the top three layers of the model will normally be referred to as the middle stratosphere, the remaining region above the tropopause being the lower stratosphere.

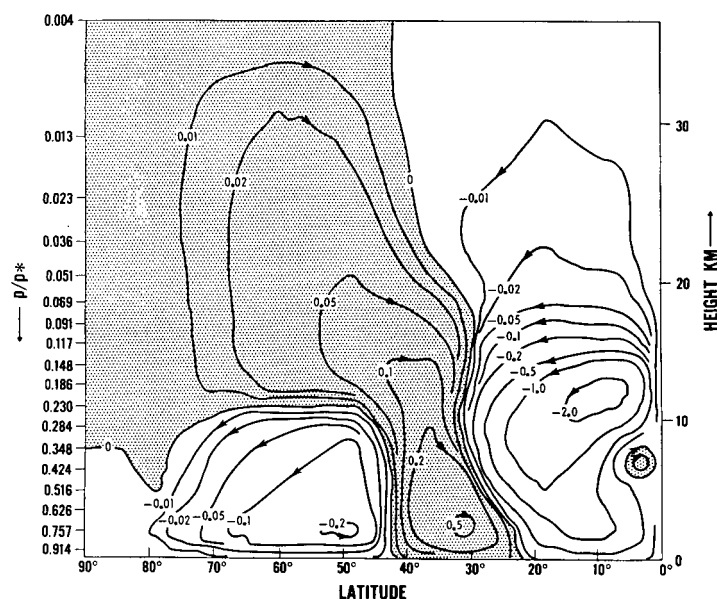


FIGURE 9.—The stream function illustrating the meridional cell structure of the model atmosphere. (Units: sec.⁻¹)

with both having about the right intensity. The polewards tilt of these winds with height is also obtained. The region of strong southerly winds in the upper tropical troposphere is also in agreement with observation, and appears to be of about the correct intensity.

The vertical velocities are fairly similar to those obtained previously except more detail is apparent in the upper levels, and rather more damage has been caused by the reverse cell in the Tropics. The maximum zonal mean vertical velocity of 1 cm./sec. was obtained in the upper troposphere at the Equator, a value which is thought to be somewhat larger than that occurring in the atmosphere. It can be seen that the Tropics was a region of general upwards motion at all levels, while the subtropics received the associated downwards motions.

Although an approximate idea of the cellular structure of the model atmosphere can be obtained from the velocity distributions, a much improved picture is given by the stream function shown in figure 9. This figure was derived by using the model velocities given in figure 7 to define the relative vorticity, and then solving the Poisson equation for the vorticity to obtain the stream function. Some smoothing of the velocities was inevitable in this procedure so that the reverse cell in the Tropics is probably underestimated. The 3-cell structure usually associated with the troposphere is clearly shown, as is the transition to 2 cells in the stratosphere which results from the squeezing out of the high latitude direct cell. Although the indirect cell is rather small in the troposphere it predominates in the stratosphere, and a feature of interest is that most of the polewards transport associated with this cell at higher levels is confined to a rather thin layer in the lower stratosphere. The tropopause appears to have little effect on the direct cell in the Tropics, and while its maximum transport is confined to the troposphere, the cell clearly penetrates to high levels. The combination of both stratospheric cells to give downward motion in the subtropics should also be noted. Miyakoda [24] has

TABLE 2.—Approximate intensity of meridional circulation (units: 10^{12} gm./sec.)

	Calculated			Observed		
	Dry 18-level model	Dry 9-level model	Moist 9-level model	Palmén and Vuorela [32]	Mintz and Lang [23]	
	Annual mean	Annual mean	Annual mean	Winter	Winter	Summer
Direct cell in the Tropics.....	98.2	52	140	230	85	40
Indirect cell in middle latitudes..	19.8	46	23	30	27	30

also deduced a 3-cell tropospheric and a 2-cell stratospheric system based on an observational study of the atmosphere. He found that the high latitude stratospheric indirect cell was maintained by the adjacent tropospheric direct cell, however his more recent studies (personal communication) have resulted in a similar structure to that given in figure 9, except that the zero line in the stratosphere was at about 55° lat. The cellular structure in the stratosphere is of considerable importance in the transport of tracers, and this aspect will be discussed in more detail in Part II [7].

In table 2 the intensities of the direct and indirect cells of the troposphere are compared with observation and with previous models, and it can be seen that the present model agrees fairly well with the results of Mintz and Lang [23] for winter conditions.

5. ANGULAR MOMENTUM BALANCE OF THE ATMOSPHERE

In this section it is not intended to discuss how the angular momentum balance of the atmosphere is maintained as the 18-level model has little to add in this regard. The purpose here is to point out the damage caused by the reverse cell in the Tropics, which severely affected the angular momentum transport in the model. Now it is known from the observational studies of Starr and White [38] and confirmed by the 9-level model of S, that the eddies in the atmosphere are primarily responsible for transporting angular momentum from the Tropics polewards. This transport is maximum at a height of about 12 km. and is polewards at least to about 60° lat., north of which weak, but not negligible, equatorwards transport appears to exist. In the case of the present model, as shown in figure 10, there is extensive equatorwards transport in the upper troposphere at all latitudes with a maximum at about 40°, and this is now as large as the northward eddy flux which usually maintains the jet stream. The influence of the reverse cell in the Tropics is seen by the extension of the equatorwards transport into this region, which severely reduces the normal polewards flux in the troposphere. As a result the tropospheric jet stream in the model tended to be pushed equatorwards, thereby accounting for its location at 27° lat. In the middle stratosphere of the model there is a local maximum in the polewards

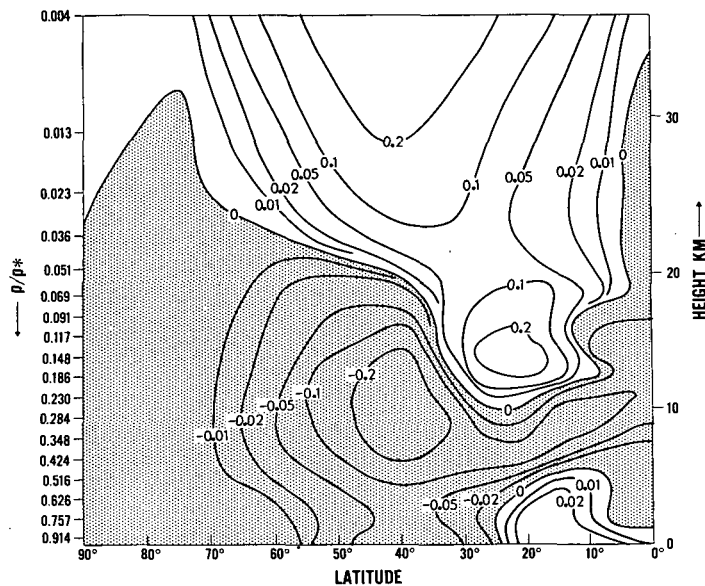


FIGURE 10.—The latitude-height distribution of the computed northward flux of angular momentum by large-scale eddies. Shaded areas are regions of equatorwards flow. (Units: 10^{27} gm. $\text{cm}^2 \text{sec}^{-2} \text{atm}^{-1}$)

transport of the angular momentum by the large-scale eddies which did not exist in the 9-level model, and this served to maintain the angular momentum of the high-level jet stream.

In figure 11 the convergence of the angular momentum flux by the large-scale eddies is given. This was found to be in closer agreement with the results for the 9-level model than was the case for the corresponding eddy fluxes. Compared with the 9-level model the intensity of the divergent poleward region has increased by a factor of five and there has also been a general weakening of the convergent areas. The divergence due to the meridional circulation was almost equal and opposite to that shown in figure 11 for the eddies except in the lower troposphere where the vertical mixing of momentum predominates, so that a steady state had been reached in the momentum balance.

Despite the unconventional manner in which the angular momentum of the jet stream was maintained, its major consequence appears to be only a general southwards trend of the features in the troposphere. The basic meteorological fields given in the previous section are all thought to be representative of atmospheric conditions, and it is not considered that any of the results presented here or in Part II would be noticeably changed if a more normal angular momentum balance had existed. This balance does, however, indicate the need for careful analysis of the results of a general circulation experiment, as it is quite possible to get the right result for the wrong reason.

Note, although the distortion of the angular momentum balance has been attributed to the reverse cell in the Tropics, it is not entirely clear that it is the only cause of this trouble. The rather crude formulation of the boundary layer is another possible cause, as this influenced the extent of the vertical momentum mixing from the surface. In this respect the 9-level model was superior; however, it also had a reverse cell. Hence, the possibility exists that some other mechanism in the model may be

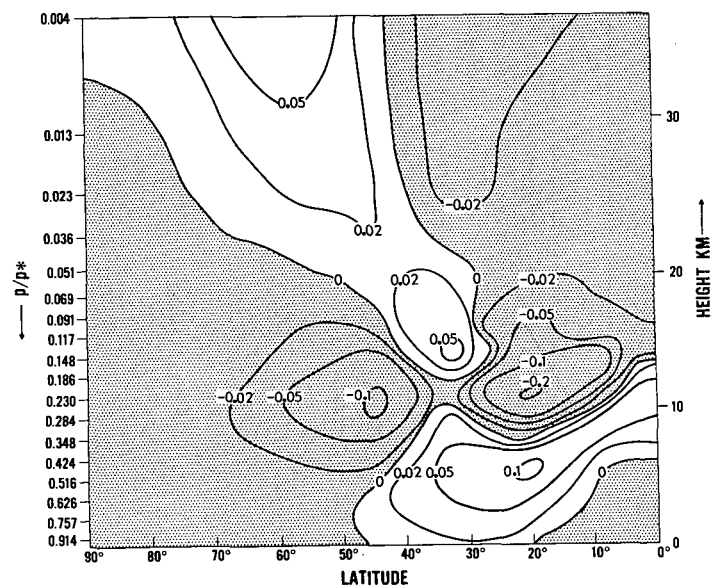


FIGURE 11.—The latitude-height distribution of the rate of change of angular momentum produced by the large-scale eddies. Shaded areas are regions where the angular momentum is decreasing. (Units: $10^7 \text{ cm}^2 \text{sec}^{-2}$)

causing the trouble, and at the present time further investigations are underway.

6. HEAT BALANCE OF THE ATMOSPHERE

A complete description of the heat balance of the atmosphere will not be attempted here as many of the aspects involved, particularly for the troposphere, have been adequately discussed previously by *S*. Accordingly attention will be primarily confined to the stratosphere, but in order that the results presented may be viewed in the correct perspective, the following general background is provided.

The ultimate source of energy for the atmosphere is solar radiation, which heats both the atmosphere and the earth's surface by absorption. The absorption in the atmosphere varies quite markedly with altitude, following the latitudinal variation of the incoming radiation and the vertical distribution of cloud, water vapor, carbon dioxide, and ozone. For an atmosphere in radiative equilibrium, where the temperatures are obtained as a balance between the long wave and short wave radiations, a rather unrealistic situation results. In general the atmospheric temperatures are somewhat low, and high lapse rates are obtained in the layers adjacent to the surface; in addition there is a large latitudinal temperature gradient because of the smaller insolation at high latitudes. These lapse rates produce dry or moist convective instability, with the result that the surface temperatures are reduced while the troposphere is warmed. Because of the higher surface temperatures in the Tropics, moist convective activity is of greatest importance there and extends to the height of the tropopause, but at higher latitudes less energy is available to support large-scale convective activity and there is a steady reduction in the importance of this mechanism as one progresses polewards (see figure 5.D.2 of *S* and figure 12c1 of Manabe et al. [19]). Thus the marked latitudinal temperature gradient in the troposphere produced by the

solar radiation remains even for an atmosphere in radiative-convective equilibrium, and it is this heat imbalance which is the fundamental cause of the general circulation. Since this temperature gradient also corresponds to a pressure gradient, an accelerating force exists and this generates large-scale dynamical motions by which the general circulation attempts to remove the imbalance by transporting latent, as well as sensible, heat from low to high latitudes. At all latitudes the long wave radiation is generally opposing this heating of the atmosphere, as it is trying to return the atmosphere to the lower temperatures associated with the radiative equilibrium state. Hence as a result, a quasi-steady state is obtained in which the various heating terms balance one another.

The situation at higher levels in the atmosphere is somewhat different, as convection ceases to be of importance, while forcing by the troposphere is a factor which has to be allowed for, and this is one of the aspects which will be discussed subsequently.

6.1. LATITUDE-HEIGHT DISTRIBUTION OF HEAT BALANCE COMPONENTS

In figure 12, the radiation fields with which the general circulation interacts are shown for zonally averaged conditions. The solar and long wave radiation fields were obtained by inserting the 100-day mean latitude-height temperature distribution into a radiative scheme as used in the model, whereas the net radiation field was taken as the 100-day mean of the radiative temperature tendency generated by the model. These results are in general agreement with the work of London [16] for the actual atmosphere, and with other computations of the heat balance of the atmosphere such as those carried out by Ohring [30] and Manabe and Möller [18], amongst others. The solar radiation heating has a latitudinal gradient at all altitudes except in the vicinity of the tropopause, the minimum heating rates being at high latitudes following the variation of the insolation, another minimum occurring around the tropopause where both the ozone and water vapor concentrations become rather small. In the middle stratosphere there is a rather high heating rate at all latitudes. The long wave cooling rates in general tend to follow a pattern very similar to the solar heating rates, except that their magnitudes are larger in the troposphere, especially in the Tropics. A point of interest in the present results is the region of long wave heating which occurs in the vicinity of the tropical tropopause, a feature not obtained in the 9-level model and which will be discussed later. Heat balance computations by Kennedy [10] using observed atmospheric properties also indicate a similar small heating due to long wave radiation. The total heating rate given in figure 12 reveals that, apart from a region of the tropical stratosphere, there is a net cooling at all locations. This is a well-known result, but it is important since it reveals that practically the whole of the atmosphere is heated indirectly by convection from the surface followed by large-scale transport of this convective heat. In the actual atmosphere it is moist convection and the resulting heat of condensation which are principally responsible for

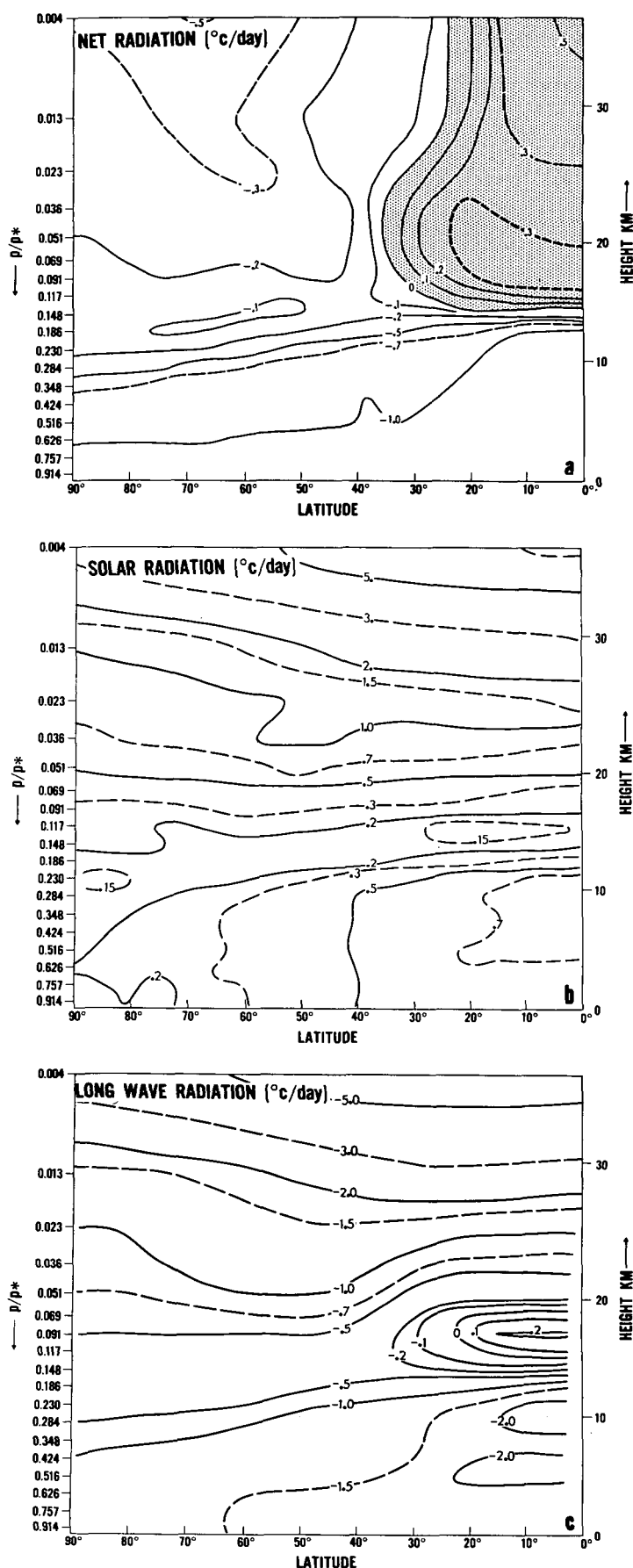


FIGURE 12.—The latitude-height distribution of the calculated rate of temperature change due to the net radiation, the solar radiation, and the long wave radiation are shown in the upper, middle, and lower parts of the figure, respectively.

compensating this cooling, the present model, however, does not incorporate these mechanisms explicitly, but they were replaced by the simple process of convective adjustment. The region of maximum cooling is the troposphere, which indicates that it is there that the atmosphere is furthest from radiative equilibrium. On the other hand the middle stratosphere (above about 30 mb.) is fairly close to radiative equilibrium, since the total cooling rate is very small compared with the solar and long wave rates.

In figure 13 observed (Starr and co-workers) and calculated large-scale eddy fluxes of sensible heat are compared. The horizontal eddy fluxes agree particularly well with the annual mean transports, even though they are slightly too far south, following the general trend of this model. Unlike the 9-level model two regions of maximum flux are obtained at midlatitudes, one in the troposphere, the other in the middle stratosphere. In agreement with the observations of Starr and Wallace [39] the model has a weak horizontal countergradient flux in the tropical troposphere. However, the area of equatorwards flow in the immediate vicinity of the tropical tropopause, which is not shown by the observations in figure 13, is downgradient transfer supplying heat to this very cold region. Up to about level 4 ($p/p^*=0.036$) in the stratosphere at midlatitudes the horizontal flux is also countergradient, although it is only strongly countergradient in levels 6 and 7, a result first obtained by White [43] for the actual atmosphere and by *S* and Peng [33] for model atmospheres. In the model very weak countergradient heat flux also exists in the lower stratosphere at high latitudes, and this is probably indicated for the observed results in figure 13 by the extremely weak equatorwards flow in this region. The large northward eddy heat flux in the middle stratosphere predicted by the model is considerably greater than that given by Wallace [42] based on a rather limited observational region. Wallace's data are not included in figure 13 as they seem to be too small at all altitudes; in the region where they overlap the 5 yr. of data of Starr's group they are about a factor of two smaller while, at 10 mb. they are four times smaller than the model results. Part of this discrepancy might be due to Wallace having only computed transient eddies. Qualitatively, however, the agreement with the model is excellent, as Wallace computes very small fluxes south of 30° lat. and a distinct maximum at about 50° at a height of 10 mb., the highest level he considered.

No vertical eddy heat fluxes are included for comparison with the computed values in figure 13 since only fluxes derived using adiabatic vertical velocities are available, and these are not considered to be very accurate. Nevertheless the results of Jensen [8] obtained in this manner for a rather limited region are in reasonable agreement with the computed values. The dominant feature of the vertical fluxes is the upwards transport in the middle troposphere ($p/p^*=0.516$) at extratropical latitudes, which helps to supply heat to the cold upper troposphere. This vertical eddy flux is actually countergradient since it is transferring heat towards a region of warmer potential temperature, even though it has a lower sensible

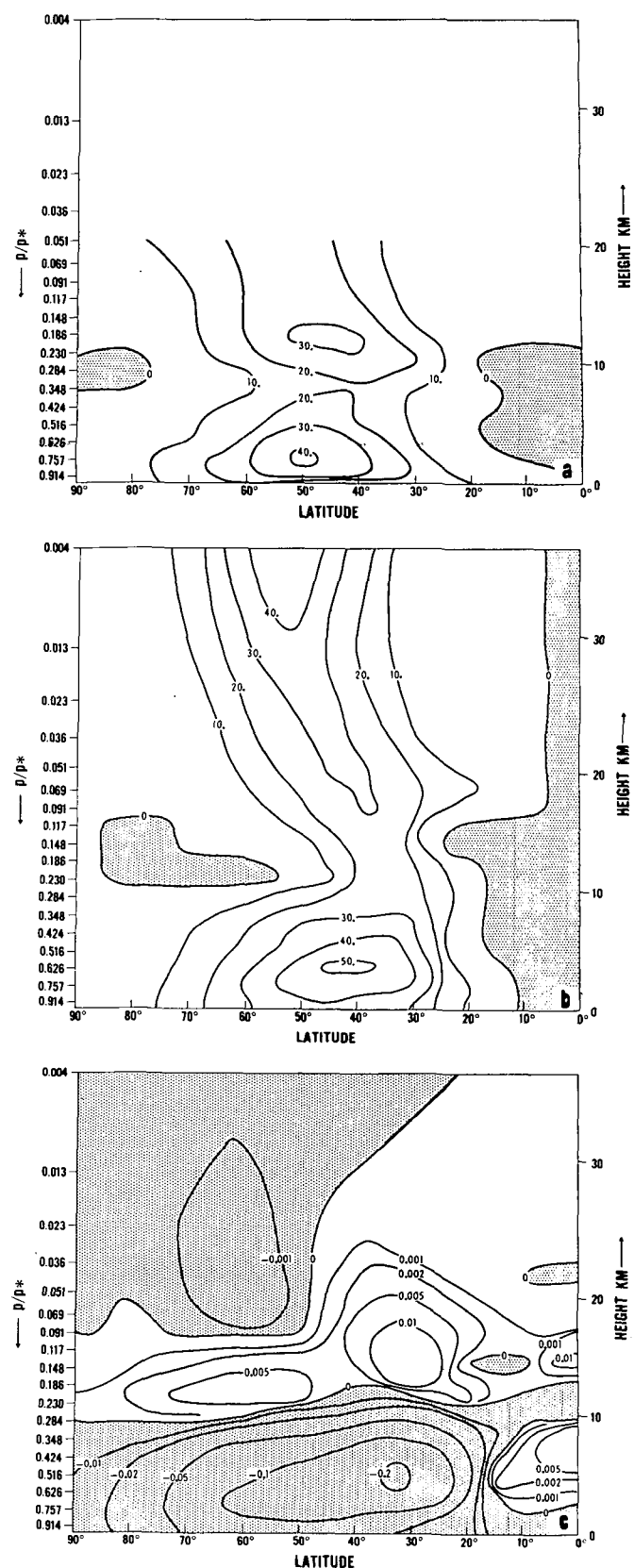


FIGURE 13.—The latitude-height distribution of the northward flux of heat by large-scale eddies (units: 10^{21} ergs atm. $^{-1}$ sec. $^{-1}$) for observed and computed conditions are given in the upper and middle parts of the figure respectively. The observed flux due to Starr and co-workers contains the contributions of both standing and transient eddies. In the lower part of the figure the computed vertical heat flux on the isobaric surface due to eddies is shown. Shaded areas are regions of upwards or equatorwards flow. (Units: 10^6 ergs cm. $^{-2}$ sec. $^{-1}$)

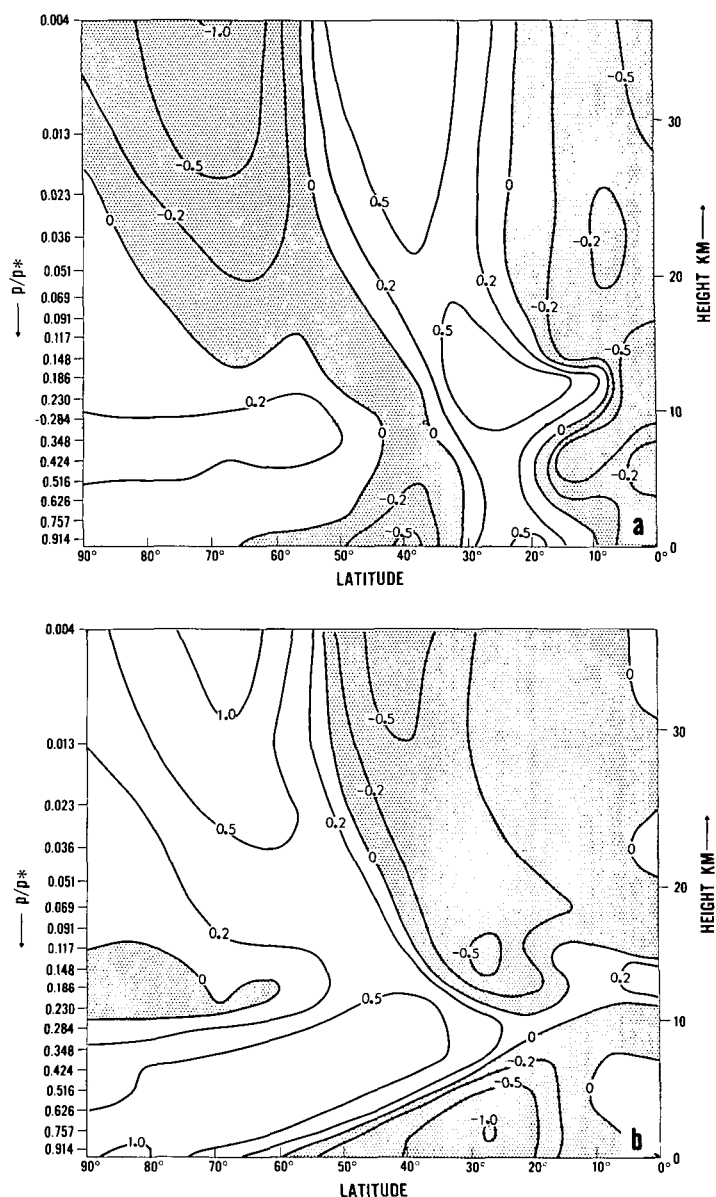


FIGURE 14.—The latitude-height distributions of the rate of change of temperature due to the meridional circulation and the large-scale eddies are shown in the upper and lower parts of the figure respectively. Shaded areas are regions where cooling is taking place. (Units: °C./day.)

temperature. The total eddy flux is such that heat is transferred upwards and polewards in the troposphere by the baroclinically unstable waves, as predicted by Charney [3] and Kuo [12]. In the lower stratosphere the waves are generated by the action of the troposphere and heat is transported downwards and polewards in the model, in agreement with the observation of Newell [27].

Finally figure 14 shows the rate of temperature change produced by the heat fluxes associated with the mean meridional cells and the large-scale eddies. Unlike the troposphere, it appears that in the model stratosphere, particularly at the upper levels, the eddies and meridional cells produce virtually compensatory changes. This appears to be a characteristic feature of the motions in the stratosphere, and will be seen again when the tracers

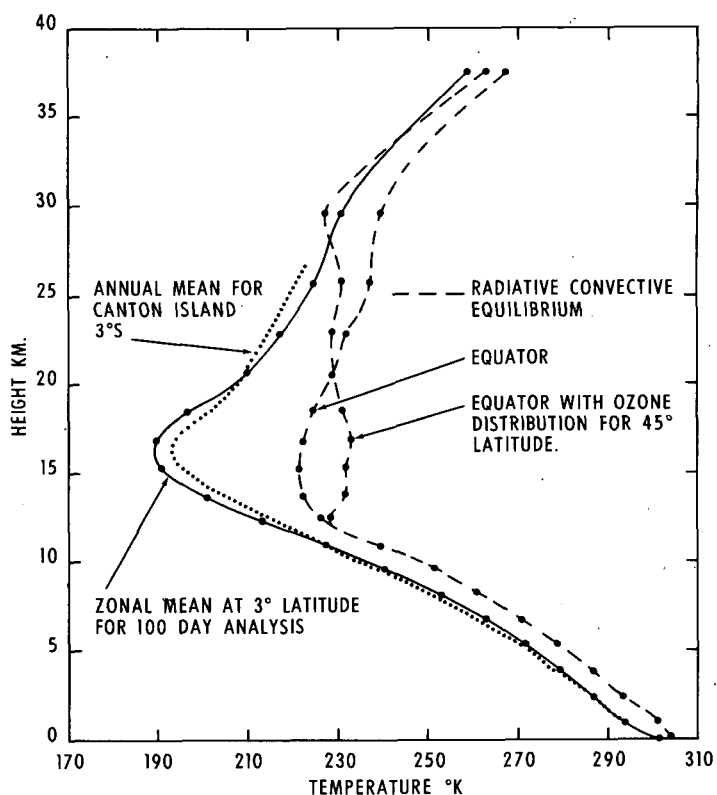


FIGURE 15.—Comparison of computed and observed tropical temperature profiles. The radiative-convective equilibrium profiles show the temperature distributions which are obtained when the influence of the large-scale dynamics is omitted.

are discussed in Part II. The temperature tendencies will be analyzed in more detail in a later section.

6.2. VARIATION OF THE VERTICAL TEMPERATURE PROFILE WITH LATITUDE

Having disposed of the description of the basic heat balance components, one is interested to investigate how they interact to produce the observed variation of temperature in the atmosphere. This raises a number of fundamental questions such as: Why has the equatorial vertical temperature profile so sharp a minimum at the tropopause? Why does the shape of the vertical temperature profile change with latitude? Why does the height of the tropopause vary with latitude, and what is the reason for the existence of the tropopause gap? An attempt will be made to answer some of these questions in this section.

6.2.1. *Tropics.*—In figure 15 the zonal mean model temperature at 3° lat. is compared with the annual mean temperature profile for Canton Island 3°S., an individual station rather than a zonal mean being used for reasons discussed previously. The agreement between the computed and observed profiles could hardly be improved and is a very encouraging feature. Also shown in the figure are two equatorial temperature profiles which were calculated independently of the model for radiative-convective equilibrium conditions (see Manabe and Strickler [20]). One profile was calculated for a typical tropical distribution of ozone, while the other was obtained using the ozone concentrations at 45°N. According to this comparison the lower ozone concentrations of the Tropics

reduced the temperature of the tropopause region and tended to accentuate the sharpness of the tropopause, but were not sufficient to simulate quantitatively the sharpness of the actual tropical tropopause. The most interesting feature of this figure however is the difference between the equatorial radiative-convective temperature profile and that given by the model, since this illustrates the very important changes produced by the incorporation of the large-scale dynamics. Throughout the atmosphere a cooling has occurred because the Tropics export heat towards higher latitudes, as mentioned previously. The largest cooling was in the vicinity of the tropopause where the temperature fell by 30°K ., resulting in a sharpening of the temperature profile and a rise in the tropopause height of about 5 km.

A breakdown of the various quantities involved in the maintenance of the model temperature profile is given in figure 16. This shows that over most of the troposphere the heating is almost entirely due to convection from the surface, and, since this produces temperatures which are larger than those obtained for radiative equilibrium, the radiation is working very hard to cool the troposphere, despite the temperatures having already been reduced by the dynamics below those for radiative-convective equilibrium. The radiative cooling reaches a maximum at about 10 km., as cooling to space is most effective there. This tends to result in unstable lapse rates, which accentuate the small-scale convective activity and produce a concurrent maximum in the convective heating. Figure 16 also reveals unequivocally that it is the mean meridional circulation which is responsible for the sharpness of the temperature profile in the Tropics, since this is virtually the only large-scale dynamical effect operative in this region. The meridional circulation achieves this by the adiabatic cooling associated with the upwards motion which the model has at all altitudes in the Tropics, the variation of the cooling rate with altitude following from the corresponding variation of the upwards velocity shown in figure 7. Near the tropopause and in the lower stratosphere the upwards velocity decreases as the static stability increases, and, although this reduces the dynamical cooling rate, the largest reduction in the temperatures shown in figure 15 occurs in this region. This is because the heating rate decreases faster, and not only is the solar heating extremely weak there, but the convective heating disappears owing to the stable stratification. As a direct consequence the only way the adiabatic cooling can be compensated for is by the long wave radiation providing a net heating in the vicinity of the tropopause, and this is the reason for the very rapid change of sign of the radiation term there in figure 16. Obviously the radiative components are very finely balanced at this location, but the contribution to the radiative heating by long wave absorption by carbon dioxide is in fact greater than that by absorption of solar radiation by all three absorbers. In order for this long wave heating to exist it is necessary to have a sharp temperature minimum, as under these circumstances the region near the minimum receives more emission from the adjacent warmer layers than it can emit because of its low black body temperature. This

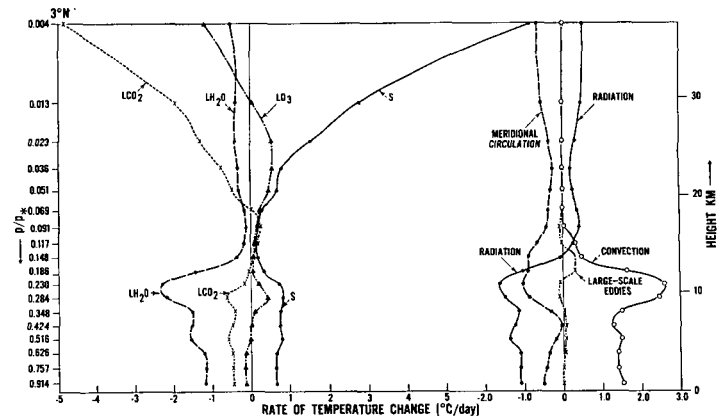


FIGURE 16.—The vertical distribution of the various heat balance components in the Tropics. S gives the rate of temperature change due to absorption of solar radiation by water vapor, carbon dioxide, and ozone. LH_{2O} , LCO_2 , and $L03$ give the individual contributions to the rate of temperature change due to long wave radiation of water vapor, carbon dioxide, and ozone respectively.

explains the limitation of the long wave heating in figure 12c to the vicinity of the tropical tropopause. At higher levels in the stratosphere absorption of solar radiation by ozone provides an increasingly important heating contribution because of the increasing ultraviolet radiation, while the long wave component of carbon dioxide returns to its cooling role. A net radiative heating is still required, though, in order to compensate for the meridional cooling, and this accounts for such heating shown in the tropical stratosphere in figure 12a. At higher latitudes the dynamics produce a net heating in the stratosphere, and the more usual situation of a net radiative cooling exists there. The results in Part II reveal that the ozone distribution in the Tropics is influenced by the vertical motion associated with the direct cell, and the meridional circulation therefore also helps to promote the temperature inversion via this influence.

6.2.2. Higher latitudes.—Considering now conditions at higher latitudes, one is interested to contrast the distribution of the heat balance components with that existing in the Tropics, and this has been done in figure 17 for two latitudes representative of two other types of temperature profiles in the atmosphere. Dealing first with 75° lat., figure 5 indicates that compared with the Tropics the troposphere is considerably colder, but an extensive isothermal height range exists in the lower stratosphere which is warmer than the tropical tropopause region. Because of the low surface temperature at the higher latitudes, convection is negligible and the principal source of heat for the troposphere is transport by the large-scale eddies; hence, the roles of convection and large-scale eddies have been reversed between the Tropics and the higher latitudes. Similar to the behavior of the convection in the Tropics the contribution of the large-scale eddies falls off practically to zero at the tropopause, but unlike the convection it becomes quite large again at higher levels. The reason for this minimum may be connected with the fact that the lower stratosphere polewards of about 45° tends to be quasi-isothermal, as can be seen approximately from figure 3. Because of this, the eddy

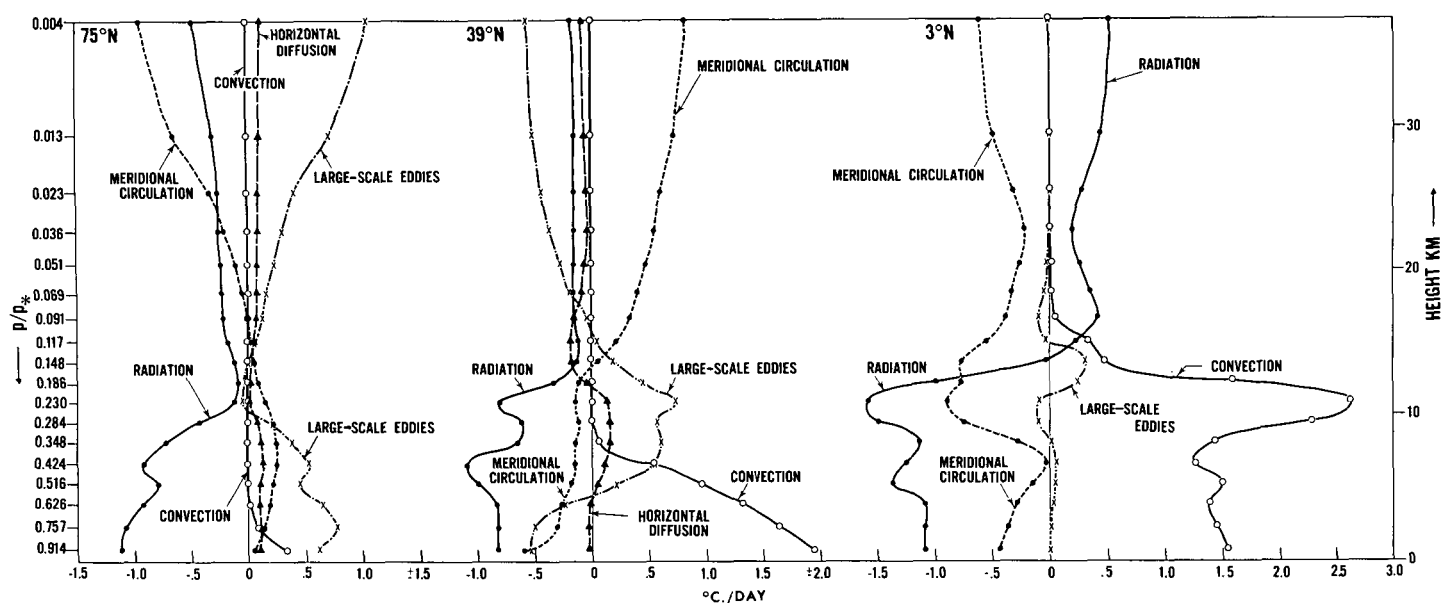


FIGURE 17.—The vertical distribution of the various heat balance components at three different latitudes. (Units: °C./day.)

heat flux is quite small, even though the “eddy activity,” as judged by the distribution of the eddy kinetic energy given in figure 23, is fairly similar to that of the troposphere. However, the troposphere has a distinct latitudinal temperature gradient which permits the eddies to transport heat polewards; similarly at higher levels in the stratosphere the eddy heat flux increases again because of the existence of a largely solar maintained temperature gradient.

The creation of the isothermal height range in the lower stratosphere at higher latitudes can partly be attributed to the corresponding ozone distribution. Figure 15 indicates that even the distribution for 45° lat. can produce such a region for radiative-convective equilibrium conditions. The effect of the large-scale dynamics on this basic temperature profile is to raise the temperature of the isothermal region, as revealed by the radiative cooling in figure 17 at 75° lat. without greatly distorting the shape. One might have expected the temperature to increase quite rapidly with height at the upper levels where the heating by the large-scale eddies is large; the reason why this does not happen is discussed in the following section. One of the important factors in maintaining the temperature in the lower stratosphere and this is the long wave radiative flux received from the middle stratosphere and particularly the troposphere. Manabe and Strickler [20] have shown that provided the troposphere has a realistic temperature structure then this will result in an isothermal region being obtained in the lower stratosphere. This therefore indicates that the heating by the large-scale eddies in the troposphere is indirectly of great consequence to the temperature in the lower stratosphere.

6.2.3. Tropopause gap.—The situation in the region of the tropopause gap remains to be considered, and conditions there are indicated by the curves for 39° lat. in

figures 5 and 17. A rather hybrid state exists there compared to the other latitudes, both as regards the temperature profile and its maintenance, but most of the details concerning how the former arises should be comprehensible from the previous discussion. Compared with higher latitudes the large-scale eddies are very important in the vicinity of the tropopause. They supply sufficient heat to counteract the meridional cooling in the upper troposphere and are largely responsible for the diffuse quasi-isothermal structure which exists in the region of the gap. This meridional cooling is produced by the upwards branch of the indirect cell at those latitudes (see fig. 9).

6.2.4. Tropopause height variation.—Finally, mention should be made of the reason for the variation of the tropopause height with latitude, and the existence of the associated tropopause gap. Connected with these questions is the basic problem of why a tropopause exists at all in the atmosphere. The latter problem cannot be adequately answered here, but to a large extent, especially at extratropical latitudes, the tropopause height is inherent in the vertical distribution of the absorbers. Both ozone and water vapor are well known to have sharp changes in their vertical distributions at the tropopause, and it can be shown (see Manabe et al. [19] for water vapor and Part II [7] for ozone) that this is a natural consequence of the dynamic and thermal structure of the atmosphere. Actually, since the ozone and water vapor concentrations are important in determining this structure, the problem is more complex than that considered in these experiments, as they made use of fixed climatological distributions of these gases for the model radiative calculations. Although the use of climatological data represents a rather unsatisfactory state of affairs, the model results do indicate the essential underlying unity which exists between the gas concentrations and the basic structure of the atmosphere.

However, accepting the observed distributions of ozone and water vapor, it is possible to understand the basic reason for the variation of the height of the tropopause with latitude. In order to clarify the discussion it is useful to consider first the conditions which would exist without any dynamic effects present. For this purpose the radiative-convective equilibrium calculations made by Manabe and Strickler [20] for July, in which the temperatures in the lowest 5 km. of the troposphere were set to the observed values, make a good starting point. They obtained a nearly isothermal tropopause region at all latitudes with a temperature of about 210°K., the height of the tropopause varying uniformly from 10 km. at the Pole to about 14 km. at the Equator. In fact if the observed ozone distribution in the Tropics was not modified by the relatively strong upwards motions there compared with other latitudes, one might have obtained an even more uniform tropopause height. The results of Manabe and Strickler clearly indicate that the tropopause break must be dynamically produced, and the basic function of the dynamics must be to raise the tropopause in the Tropics, while leaving the situation at extratropical latitudes essentially unchanged. The previous discussion concerning how the tropical temperature profile is maintained should leave no doubt that the dynamics involved are principally those associated with the direct cell in the Tropics. Figure 15 shows that the cooling produced by this cell raises the "radiative tropopause height" to a value in close agreement with observation, while the warming associated with the downwards branch of this cell would tend to depress the height of the tropopause around 30° lat. At higher latitudes the heating by the horizontal eddies tends to depress the tropopause height slightly. Thus from considerations of radiation and of the direct cell in the Tropics the basic features of the variation of the tropopause height can be accounted for. Although these two terms seem to be the dominant ones involved, the above discussion is somewhat superficial since the adiabatic cooling by the direct cell only extends to 15° lat. at the height of the tropopause in the model, whereas the high level tropopause extends to about 33°. The additional cooling comes from the horizontal component of the large-scale eddies which is transferring heat countergradient towards higher latitudes in this region as described previously.

6.3. TEMPERATURE DISTRIBUTION IN THE STRATOSPHERE

When meteorological observations of the stratosphere became available a puzzling feature which emerged was the variation of the latitudinal temperature distribution at approximately the height of the tropical troposphere. As shown in figure 4 it was found that in winter the highest temperature was at midlatitudes, while in summer it was at the Pole. In accordance with the temperature structure in the troposphere one might have expected the highest temperature to be at the Equator, and for there to be a monotonic temperature decrease from the Equator to the Pole. This therefore poses the question as to how such a temperature gradient is maintained, and what are the relative roles of radiation and dynamics in this process.

This question will be discussed before considering the temperature structure at high levels in the stratosphere.

The first attempts to explain this phenomenon were restricted to radiative considerations only. Among the various proposals advanced was a rather ingenious one by Dobson et al. [4] who suggested that the latitudinal maximum resulted from absorption of long wave radiation by the 9.6-micron band of ozone, because, while the surface temperature decreased with latitude, the ozone amount in the lower stratosphere increased, so that the greatest absorption of outgoing terrestrial radiation would probably occur at higher latitudes. On the other hand Goody [5] advanced an alternative explanation which accounted for the observed variations in terms of a balance between cooling by water vapor and warming by carbon dioxide due to long wave radiation in the lower stratosphere. These hypotheses required that the lower stratosphere should be in radiative equilibrium, whereas calculations by Ohring [30] showed that it was not. A clear idea of the role of radiation was finally obtained from the detailed study of Manabe and Möller [18] who investigated the contributions of the various gases in the heat balance of the lower stratosphere, and found that they also did not meet the specified requirements. This completely disposed of radiation as a possible explanation and left dynamical effects as the only likely source. An indication of the role of the dynamics had in any case been obtained earlier in the work of White [43], who found that countergradient heat transport by eddies was taking place in this part of the atmosphere.

Two previous attempts have been made to explain this problem using numerical models. *S*, as noted before, obtained results which were qualitatively in agreement with observation but concluded that their model needed further refinement to achieve better simulation. Peng [33], using a relatively simple, quasi-geostrophic, truncated harmonic model in which the static stability was fixed, which thus removed the need for an explicit radiation calculation, obtained a temperature gradient very close to that of the atmosphere. However, because of the nature of his basic assumptions concerning the static stability, a considerable part of the structure of the atmosphere was built into the model, and this somewhat limits the interest in his results.

The present model with its higher vertical resolution provides the refinement needed in the previous model, and a latitudinal temperature gradient of the correct magnitude is now obtained as indicated in figure 4. A discussion of all the terms involved in the heat balance in the lower stratosphere can therefore be given, and figure 18 presents the latitudinal distributions of these terms for level 7 (91 mb.) of the model. After considering the radiative terms first, it appears that the net radiative heating and the temperature distribution are partially out of phase, since heating is occurring only in the low temperature region in the Tropics, while there is cooling at high latitudes, and, in particular, in middle latitudes where the temperature maximum is located. This indicates that not only is radiation not responsible for the observed temperature distribution, but that it is endeavoring to

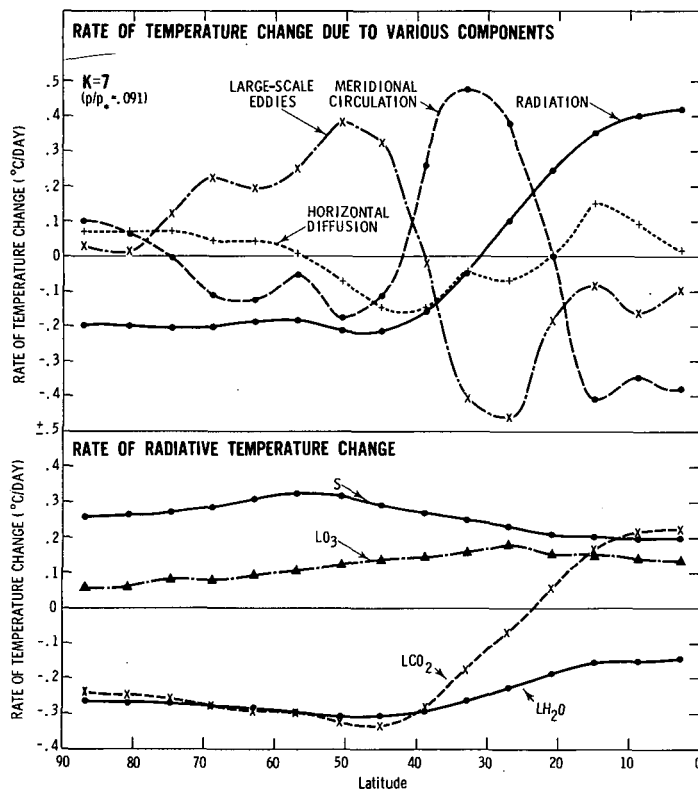


FIGURE 18.—The variation with latitude in the lower stratosphere of the various heat balance components. For further explanation refer to the caption of figure 16.

destroy the existing gradient. The lower part of figure 18 shows the contributions of the various gases and is very similar to the results of Manabe and Möller. The use of annual mean conditions in the model gives a maximum solar heating rate in middle latitudes, principally because of the variation of the ozone distribution with latitude. As required by the hypothesis of Dobson et al. [4], heating by ozone due to the absorption of long wave radiation also occurs, but the maximum heating rate is at about 25° rather than at high latitudes, indicating that the latitudinal increase of the ozone concentration is insufficient to counteract the fall in the surface temperature. No support at all is found for Goody's hypothesis, since north of 25° both carbon dioxide and water vapor are cooling the lower stratosphere.

When the dynamics are included there is no difficulty in accounting for the heat supply for middle and high latitudes. Figure 18 shows that the heat generated by the radiation in the Tropics is removed by the meridional circulation, which is simultaneously supplying heat to the subtropics. This does not mean that a direct exchange occurs between the Tropics and subtropics, as the dominant motions involved are vertical rather than horizontal. The warming in the subtropics is mainly adiabatic, because of the downwards motion associated with the direct cell, and this cell is driven by the troposphere, not by the region of radiative warming in the tropical stratosphere, which essentially balances the local meridional cooling. The subtropics are not appreciably warmed by this heat supply as the large-scale eddies, which are also forced by the troposphere, transport the heat to middle and high

latitudes, thus maintaining this region at a temperature above that for radiative equilibrium (see also fig. 14). The maximum temperatures in the model were at 45° lat. so that the southern part of the high temperature zone was also heated by the downward branch of the indirect cell. Polewards of the temperature maximum the heating effect of the large-scale eddies decreases and the temperature in this region is lower. Dynamic processes must be important throughout the year in maintaining the temperature distribution in the lower stratosphere, as Manabe and Möller [18] have shown that radiative equilibrium temperatures are never in agreement with observation.

Reference to figure 3 shows that at higher levels in the stratosphere the midlatitude temperature maximum gradually disappears and is replaced by a monotonic latitudinal gradient with the highest temperatures at the Equator. This temperature structure is similar to the radiative results of Manabe and Strickler for annual mean conditions, and indicates that in the middle stratosphere the radiation predominates over the dynamics. Figure 19 illustrates the variation with height of the various heating components, and this appears to contradict the above statement since the relative importance of the radiation decreases with altitude. This apparent paradox can be explained by comparing the radiative heating and cooling rates in figure 12 with the net radiative heating rate for the higher levels. The latter is only a small residual of the extremely large individual radiative rates, and these completely overshadow the dynamical effects and thus control the basic temperature distribution. The dynamics are therefore reduced to producing perturbations about this mean state. The gradual transition from dynamic to radiative control in the stratosphere reflects the increasing importance of ozone heating at higher levels due to the absorption of solar radiation. This is principally opposed by long wave cooling of carbon dioxide.

Returning to figure 19 it can be seen that there is a noticeable increase with altitude in the magnitude of the dynamical terms in the heat balance, and in level 1 they are surprisingly large. Basically the same dynamic processes appear to be operating at all altitudes, although there is a general northward movement in the upper levels which reflects the tilt of the horizontal eddy heat fluxes and the increase in importance of the indirect meridional circulation. An important feature of this figure is that at extratropical latitudes there is an approximate cancellation between the meridional and eddy effects, so that it is largely the difference of these terms rather than their sum which opposes the radiation. In the Tropics the eddies are virtually zero since the latitudinal temperature gradient there is very small. The dynamics do, however, produce some modification to the temperature distribution, as shown by the radiation term in figure 19 which is working to increase the Pole to Equator temperature difference in the upper levels. There is also a fundamental difference between the function of the dynamics in the middle and lower stratosphere, since in the former the dynamics are working to destroy the latitudinal temperature gradient. As a

RATE OF TEMPERATURE CHANGE DUE TO VARIOUS COMPONENTS

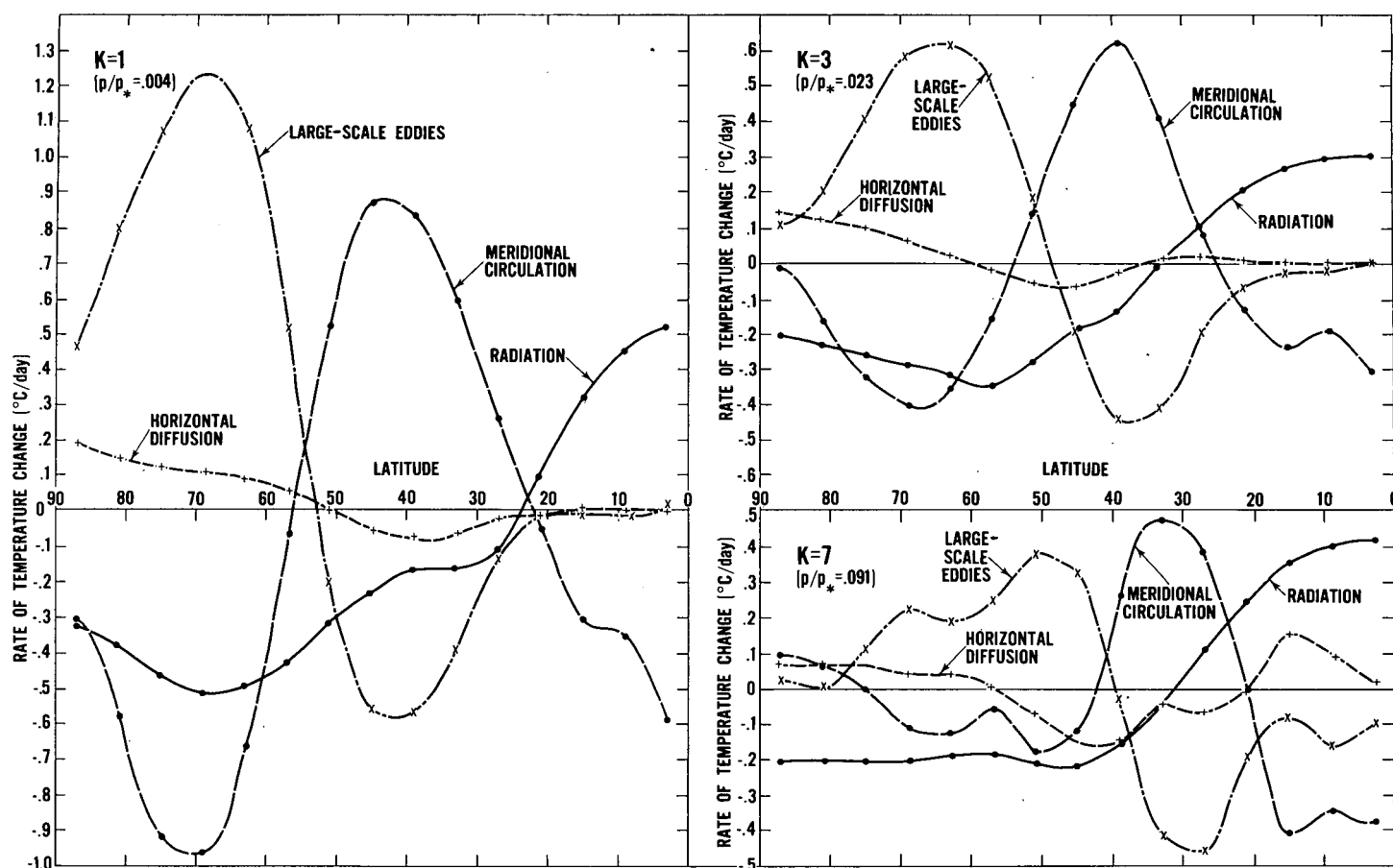


FIGURE 19.—The variation with latitude of the various heat balance components at different heights in the stratosphere.

result of this the lower stratosphere destroys zonal available potential energy, while the middle stratosphere creates it; in the parlance of Newell these regions are respectively refrigerators and heat engines.

7. MAINTENANCE OF THE WINTER STRATOSPHERE

The energy budget and transformations involved in the maintenance of the troposphere have been described in detail by *S*; hence the present discussion will be mainly limited to the stratosphere, which they were not able to deal with adequately because of their limited vertical resolution in that region.

There are some features of the stratosphere which will not be considered here because the model does not provide adequate information for a meaningful discussion. One of the most interesting of these is the 2-cell structure of the stratosphere. Why this should exist and why it is different from the 3-cell structure of the troposphere is not clear, but presumably these are fundamental features associated with the baroclinic nature of the atmosphere. Another, not unrelated, problem which also cannot be answered concerns the summer stratosphere. Why do easterly winds occur at this time in the stratosphere? How these winds are maintained and what cellular structure they involve are questions of some importance. Further, more specific questions will be raised subsequently, but in most cases it is not possible to produce an adequate answer. Although the model provides more information

than has been available previously concerning these questions, in practice it proves possible only to discuss the balance of the contributing features involved in any given situation. The model does not explain why the given features are balanced as they are, although it does go some way towards defining the problem more specifically. Clearly simulation of a phenomenon does not necessarily imply understanding.

7.1. WIND DISTRIBUTION IN THE STRATOSPHERE

In figure 6 the zonal wind distribution of the model has been given, and, confining our attention to the stratosphere, it appears that there are two aspects of interest. These are the well-defined westerly jet stream at high latitudes and the region of rather weak easterlies at low latitudes. Considering the latter first, a question arises: why do east winds exist at these latitudes when the mean meridional flow is polewards, which from considerations of the requirement to conserve absolute angular momentum should produce west winds? Figure 20 shows that the absolute angular momentum in this region is being reduced by divergence of the large-scale eddies, hence it is these eddies which are directly responsible for the production of the easterlies. This divergence is compensated for by the advection of absolute angular momentum by the weak meridional circulation in the tropical stratosphere, and also by subgrid scale horizontal diffusion. Since the latter is essentially the

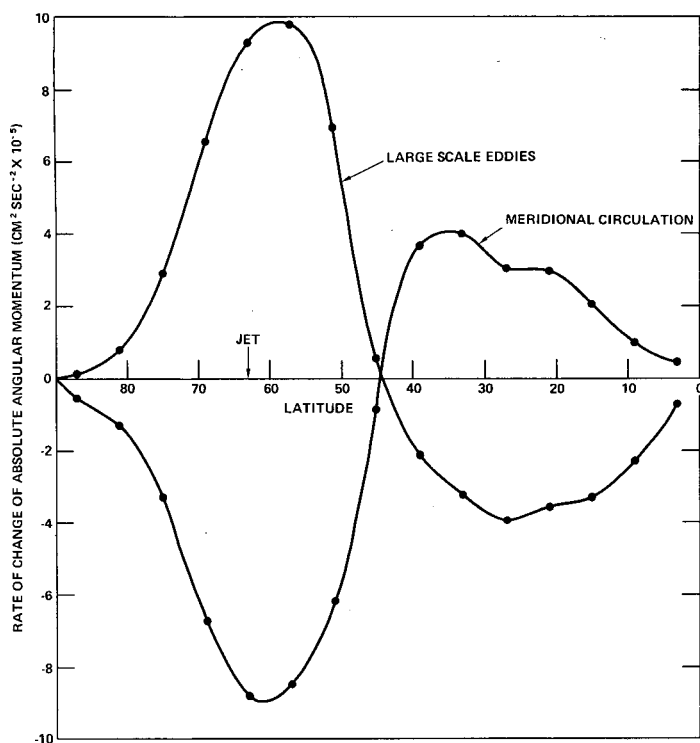


FIGURE 20.—The variation with latitude of the rate of change with time of the absolute angular momentum in the top level of the model. (Units: $10^5 \text{ cm}^2 \text{ sec}^{-2}$)

resultant of the large-scale motions, the easterlies exist because the meridional convergence is slightly less than the eddy divergence. Why this is so is unknown.

The resulting balance between the meridional circulation and the eddies is presumably rather delicate, and the biennial oscillation of the wind from east to west in this region may be related to fluctuations in the relative intensity of these mechanisms. This might then relate the cause of the oscillation to the troposphere, since the meridional circulation is driven from below. See also the discussion by Wallace [42].

After considering the high latitude jet stream in the middle stratosphere shown in figure 6, a number of questions can be posed. The most important of these is why does the atmosphere have a jet stream in this region? Also, why does it occur at 63° lat. rather than say, a latitude closer to the tropospheric jet? How is the angular momentum of the jet maintained when it is in a region where the meridional winds are equatorwards? Finally, how is the energy of this jet maintained, and what are the relative roles of local production and transport in the budget of kinetic energy?

In the case of the energy balance of the high level jet the discussion will be mainly limited to the eddy components, because of the difficulty of computing the terms involved in the generation of zonal kinetic energy on a local basis. In figure 21 the latitude-height distributions of both the conversion term of eddy available potential energy $-\overline{\omega'\alpha'}$, and the eddy pressure interaction term, $-\partial(\overline{\omega'\phi})/\partial p$, are given. These two quantities constitute the generation term of eddy kinetic energy, $-\nabla' \cdot \nabla \phi'$. The figure shows that both of these terms are supplying

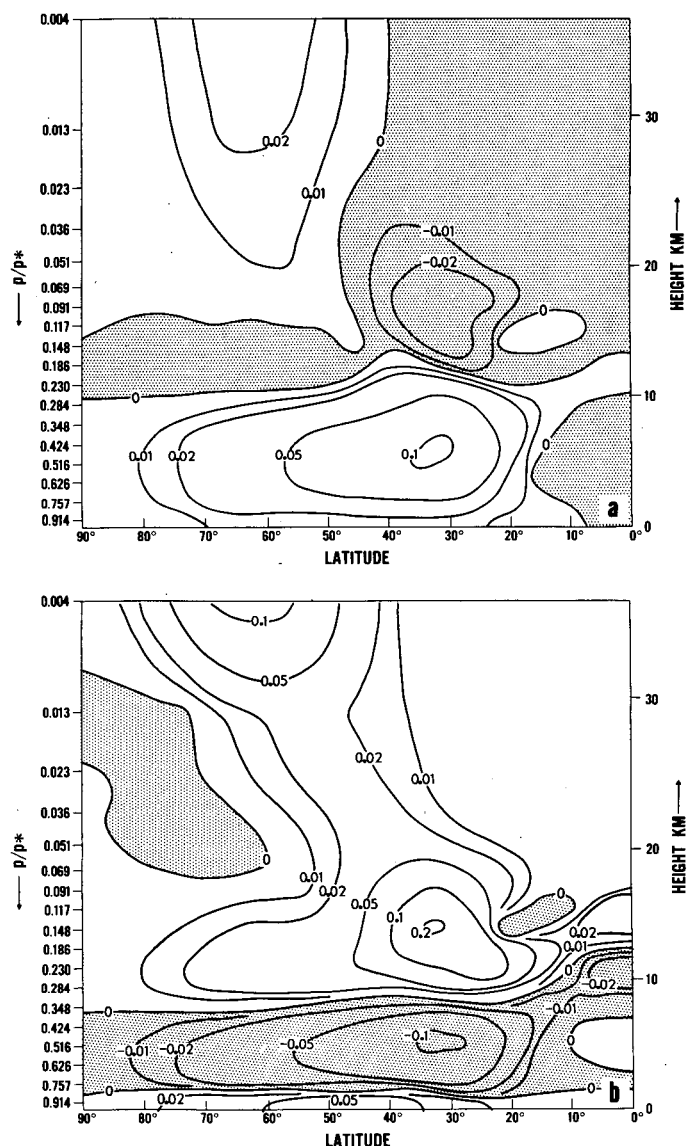


FIGURE 21.—The latitude-height distributions of the eddy conversion of potential energy into kinetic energy and the creation of kinetic energy by the eddy pressure interaction term are shown in the upper and lower parts of the figure. (Units: $10^5 \text{ ergs cm}^{-2} \text{ sec}^{-1} \text{ atm}^{-1}$)

eddy kinetic energy to the region of the high-level jet, although the $-\overline{\omega'\alpha'}$ term is much the smaller. The conversion term of available potential energy does, however, increase in the upper levels near the jet, and a similar increase in the eddy pressure interaction term can be observed in figure 21b. As shown in figure 22 this is the result of the convergence of the energy flux $\overline{\omega'\phi'}$ which originates from the troposphere, as there is a slow, but steady, decrease in this flux in the stratosphere. The distribution of eddy kinetic energy is given in figure 23 and, in agreement with the eddy pressure interaction term, has a broad maximum in the region of the upper level jet.

The downward branches of the stratospheric meridional cells would be expected to produce zonal kinetic energy around 40° lat. by means of the zonal pressure interaction term $-\partial(\overline{\omega'\phi})/\partial p$. Since the jet is at 63° lat., in the model horizontal transport of kinetic energy from the

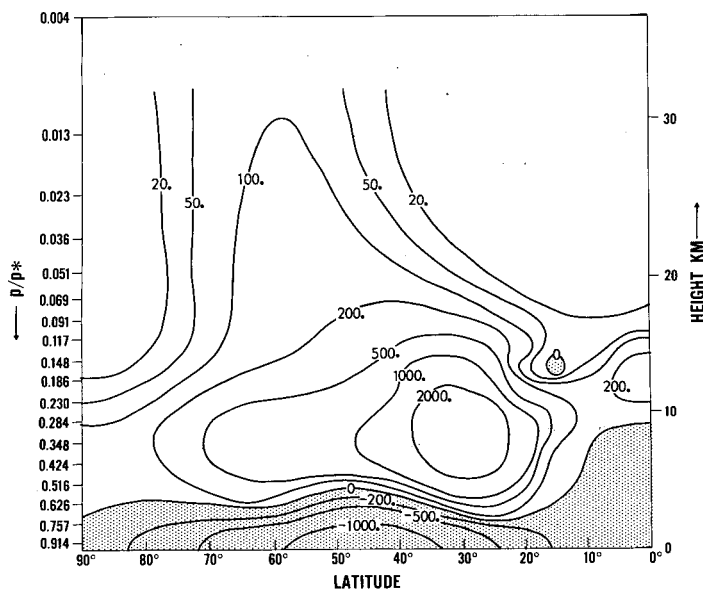


FIGURE 22.—The latitude-height distribution of the vertical flux of geopotential height $-\overline{\omega'\phi'}$ due to the large-scale eddies. Shaded areas are regions of downwards flux. (Units: ergs cm.⁻² sec.⁻¹)

source region might be expected, although this term was not computed in this study. This would then indicate that the high-level jet is not maintained locally, but requires energy from both lower levels and lower latitudes.

The above discussion still leaves the reason for the formation and location of the jet unanswered, and the situation regarding the angular momentum balance is also unsatisfactory. However, it is clear from figure 20 that it is the large-scale eddies which supply the angular momentum to the jet, and that the meridional circulation is actually removing angular momentum from the jet, because the mean meridional flow is equatorwards in this region. The meridional circulation and the large-scale eddies obviously constitute a highly interactive and compensatory system in the stratosphere as regards the angular momentum balance, and this is a feature noted previously for the heat balance in figure 19 and it will also be seen again in the tracer transports in Part II. Thus in the present model there is no inconsistency between the tracer and temperature distributions and the angular momentum balance, such as was present in previous models involving mean meridional motions in the stratosphere.

7.2. ENERGY BALANCE OF THE MIDDLE AND LOWER STRATOSPHERE

Energy box diagrams of the conventional form were constructed for the middle stratosphere, defined as the first model layers 1 to 3, 0–23.4 mb., and the lower stratosphere defined as layers 4 to 8, 36–117 mb. The choice of the lower level of the middle stratosphere was governed by the layer where the $-\overline{\omega'\alpha'}$ term changed sign. In deriving the interactions of exterior layers on these regions the energy convergences were calculated as a mean value for the whole region based on the difference between the fluxes entering and leaving that region. The results are displayed in figure 24, together with box diagrams for the 9-level model and the actual lower stratosphere as given by Oort [31]. Because of the diffi-

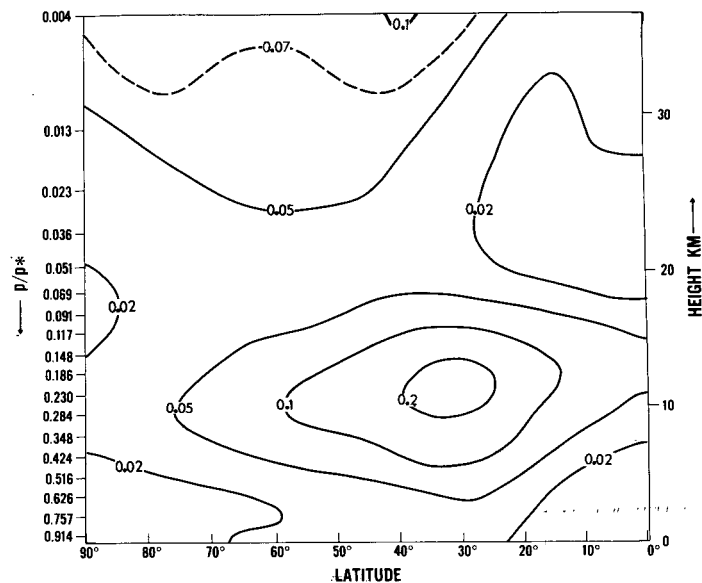


FIGURE 23.—The latitude-height distribution of the eddy kinetic energy in the model. (Units: joule/gm.)

culty of computing some of the energy exchange terms in figure 24 the boxes in general do not balance. Results for the whole atmosphere are not included since they are less realistic than those of S in one particular aspect. In the present model the K_z to K_E term incorrectly transferred energy from the zonal to the eddy flow, thus requiring K_z itself to be maintained solely by the conversion term of available potential energy. The breakdown of the K_z to K^2 term revealed that this was mainly caused by the vertical transport of momentum; the horizontal transport actually transferred energy in the correct direction. As noted previously, the angular momentum balance in the troposphere was maintained in an unusual way in this model. Hence the discrepancies in both the angular momentum and the kinetic energy conversion appear to have a common source.

Considering the lower stratosphere first, one can see that the magnitudes of the energy terms for the 18-level model show a noticeable improvement over those of the 9-level model in comparison with the results of Oort. However, there are some discrepancies as K_z and both the conversion terms of potential energy are rather large, the former being mainly caused by the tropospheric jet being too strong. The magnitudes of the generation terms of available potential energy agree better with those of Oort than previously, but the sign of the eddy generation term is still reversed. In addition the K_z to K_E term is also reversed for reasons given above. As is well known the direction of the K_E to P_E conversion is different in the lower stratosphere from that of regions on either side, and this indicates forcing of the atmosphere is taking place, which led Newell to describe this region as a "refrigerator." The kinetic energy converted to available potential energy helps to maintain the latter against radiative and dissipative losses, as the destruction of P_z by radiation is one of the principal sinks of energy in the lower stratosphere. Thus, in order to maintain this region

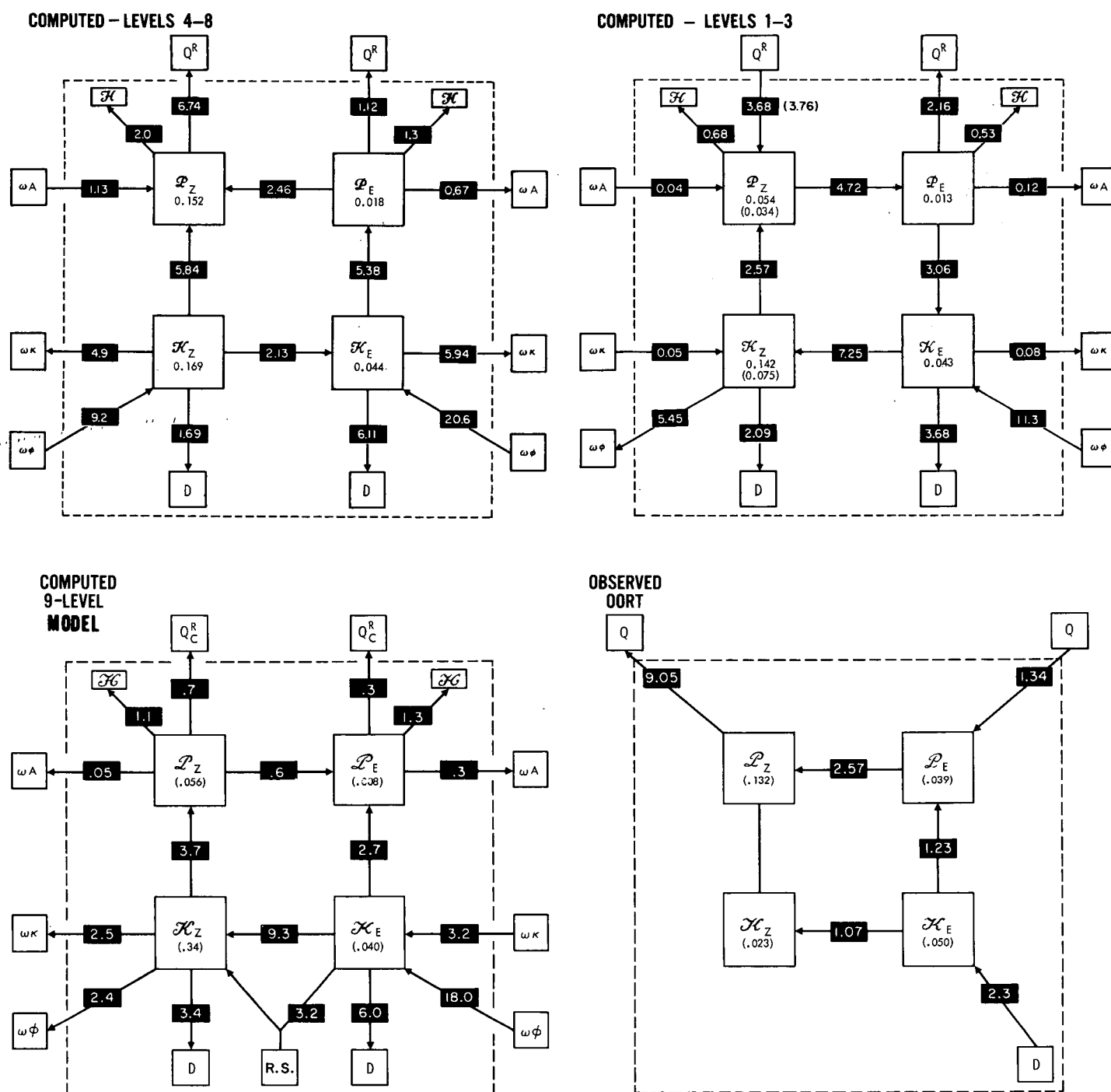


FIGURE 24.—Four box energy diagrams of the stratosphere. The upper part of the figure gives the results for the middle stratosphere (levels 1-3, 0-23.4 mb.) and the lower stratosphere (levels 4-8, 36-117 mb.) of the present model. In the lower part the corresponding results are given for the lower stratosphere (34-126 mb.) of the 9-level model and for the actual atmosphere (30-100 mb.). The energy exchange with the other layers of the atmosphere is shown by the arrows extending outside the domain enclosed by the dashed line. R.S. in the 9-level model gives the mass integral of the Reynolds stress term. The unit of energy transformation is $(10^{-3} \text{ joule}) \text{ cm.}^{-2} \text{ mb.}^{-1} \text{ day}^{-1}$, and the unit of energy is $\text{joule cm.}^{-2} \text{ mb.}^{-1}$.

it is necessary to supply energy from other regions, and the models indicate that this energy is obtained from lower levels by means of the pressure interaction term $-\partial(\omega\phi)/\partial p$; unlike the 9-level model both the eddy and meridional components of this term force the lower stratosphere in the present model. The supply of energy from lower levels is obviously of fundamental importance to the structure of the lower stratosphere, and figure 21b indicates that the exchange occurs primarily in the subtropics. Note, unlike the middle stratosphere, the vertical

transport of kinetic energy represents a significant sink of energy in the lower stratosphere.

In the middle stratosphere (0-23.4 mb.) the energy balance is maintained rather differently, and the energy cycle is the same as that of the troposphere. The vertical advection of both available potential energy and kinetic energy is of minor importance for this region, and the energy is supplied by two mechanisms. As expected from the similarity to the troposphere, one of these is the generation of P_Z by solar radiation and the other, and

more important, is again the creation of K_E by the eddy pressure interaction term which transfers energy from the lower levels. The corresponding mean meridional term is destroying K_Z in this region, and a rather large K_E to K_Z exchange is required to balance the deficit. Because of the similarity of the middle stratosphere of the model to that of the winter atmosphere it is hoped that the energy balance given here is basically correct, which would indicate that the forcing by the eddy term is a characteristic feature of this region.

The principal differences between the two stratospheric regions are that the direction of the energy exchanges involving the generation of P_Z by solar radiation, the conversion of P_Z to P_E and of P_E to K_E , and the supply of energy by $\bar{\omega}\phi$ reverse as one passes from the lower to the middle stratosphere. The most important similarities are the K_Z to P_Z conversion, the maintenance of K_E by the $\bar{\omega}\phi'$ term, and the destruction of P_E by the radiative processes associated with the large-scale eddies.

Newell [28] concluded that in winter no source of energy other than solar radiation was apparently required for the middle stratosphere, whereas in summer an inflow of energy was necessary. Newell only gave values for the three zonal terms shown in parentheses in figure 24 so that a rather limited comparison is possible. This shows that the model has about twice the magnitude for the P_z and K_z values, but about the same rate of generation of P_z by radiation; hence the atmosphere should be able to regenerate its energy much faster than the model. This however, does not prove that this atmospheric region does not import energy from other regions, since the P_z generated is mainly converted to P_E which suffers a large radiative loss and hence the net inflow of radiative energy is considerably lowered.

A comparison of the generation terms of P_E in the middle and lower stratosphere in figure 24 indicates that the efficiency of the radiative damping of P_E , and therefore of temperature fluctuations, increases with altitude. A damping factor, D , can be defined as

$$D \equiv -\frac{\frac{1}{2} G_E}{P_E}$$

where

$$G_E \equiv \overline{\gamma T' \dot{q}' / c_p}^H$$

and

$$P_E \equiv \frac{1}{2} \overline{\gamma (T')^2}^H$$

G_E is the generation term of the eddy available potential energy P_E . $(\quad)'$ denotes the deviation from the zonal mean, $(\quad)^H$ denotes the hemispheric average. T and \dot{q} are the temperature and rate of heating respectively. γ is defined on page 743 of *S*. c_p is the specific heat of air.

After using the above equations, D becomes

$$D \equiv -\frac{\overline{T' \dot{q}' / c_p}^H}{\overline{(T')^2}^H} = -\left(\frac{T'}{\sqrt{\overline{(T')^2}^H}} \right) \left(\frac{\dot{q}' / c_p}{\sqrt{\overline{(T')^2}^H}} \right)$$

This indicates that D is the covariance between the normalized temperature fluctuation $(T' / \sqrt{\overline{(T')^2}^H})$ and the

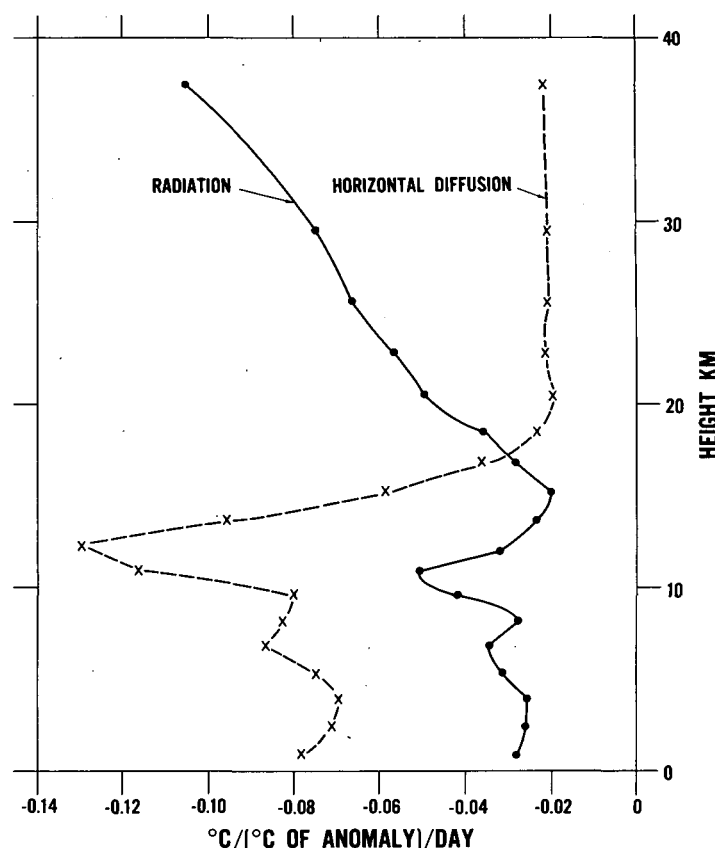


FIGURE 25.—The variation with altitude of the efficiency of damping of the temperature fluctuation by radiative and subgrid scale diffusive processes.

normalized heating fluctuation $\left(\frac{\dot{q}'}{c_p} / \sqrt{\overline{(T')^2}^H} \right)$. For the

Newtonian damping of the form

$$\dot{q}' / c_p = -a T'$$

the damping factor $D=a$ according to this equation. In figure 25 the vertical distributions of D for both radiation and subgrid scale horizontal diffusion are given, and the figure shows that the radiation damping in the stratosphere becomes of increasing importance at the higher levels, because of the approach to Newtonian cooling by CO_2 . On the other hand, the damping by the subgrid scale horizontal diffusion remains virtually constant, which explains the change in the relative importance of this term and the radiative damping in the destruction of P_E in figure 24.

7.3. SOME COMMENTS ON THE BAROCLINIC NATURE OF THE STRATOSPHERE

Most investigations of baroclinicity in the atmosphere have been confined to the troposphere, with relatively little effort having been devoted to the stratosphere. Murray [26] studied the baroclinic instability of an idealized atmosphere having a stratosphere, but he was primarily interested in the breakdown of the polar night jet. Another effort in this field has been made by Lindzen [15] who incorporated radiation as well as ozone photochemistry in his problem. He found that for adiabatic conditions

at either 30 km. or 52.5 km. the flow was unstable when the vertical wind shear exceeded some critical value, whereas when radiation and photochemistry were incorporated the flow was unstable for all nonzero shears. For simplicity baroclinic calculations usually represent highly idealized conditions in the atmosphere, and it is therefore of interest to relate the much more comprehensive results of the general circulation experiments to these calculations to see if they provide any further enlightenment on the behavior of the atmosphere.

The discussion here will be limited to the first three layers of the model since for this region the flow on a hemispheric basis was potential energy releasing, $-\overline{\omega'\alpha'} > 0$, and this is one of the requirements of baroclinicity. The present model does not include the photochemistry and advection of ozone incorporated by Lindzen in this study, and the radiative calculations are therefore based on fixed climatological ozone concentrations. As shown previously the model does, of course, have radiative damping. Unfortunately Lindzen found that the advection of ozone at 30 km. was important in his stability analysis, the major term being the vertical derivative of the ozone mixing ratio. The ozonesonde observations of Hering and Borden [6] indicate that above 25 km. a uniform mixing ratio can usually be expected, whereas Lindzen based his calculations on photochemical ozone amounts, which would account for the large vertical derivative he appears to have computed. If this is the case, then the photochemistry of ozone is probably of minor importance as a source of instability in the middle stratosphere, which would presumably modify Lindzen's stability curve somewhat. Thus it is thought that the omission of this mechanism from the general circulation model should not affect the stability characteristics of the upper levels. However, a more comprehensive investigation of this problem incorporating both photochemistry and radiation is desirable, in which the oversimplifications, particularly of the vertical structure, involved in Lindzen's approach, are removed in order to assess realistically this problem.

To provide some background a brief description will now be given of the development of the flow pattern in the middle stratosphere. As mentioned previously the model was started from conditions of zonal symmetry, and a random temperature perturbation was applied at each point after 5 days to trigger baroclinic instability. Although this produced the desired effect in the troposphere, very little response appeared in the top few levels, even though a well-defined vertical and horizontal wind shear existed in the vicinity of the upper level jet. The hemispheric variation of some of the meteorological terms of interest at 80 days in level 1 is shown in figure 26a, and this reveals that both temperature and geopotential height fields were fairly symmetrical at this time, while the polewards eddy flux of heat would be expected to be rather weak. Subsequently the development appeared to proceed somewhat faster, and the flow fields at 140 days given in figure 26b show the amplification of the westerly wave, and differ considerably from those in figure 26a. Of particular interest is the elongation of the "polar vortex," and the noticeable increase in the polewards flux of heat

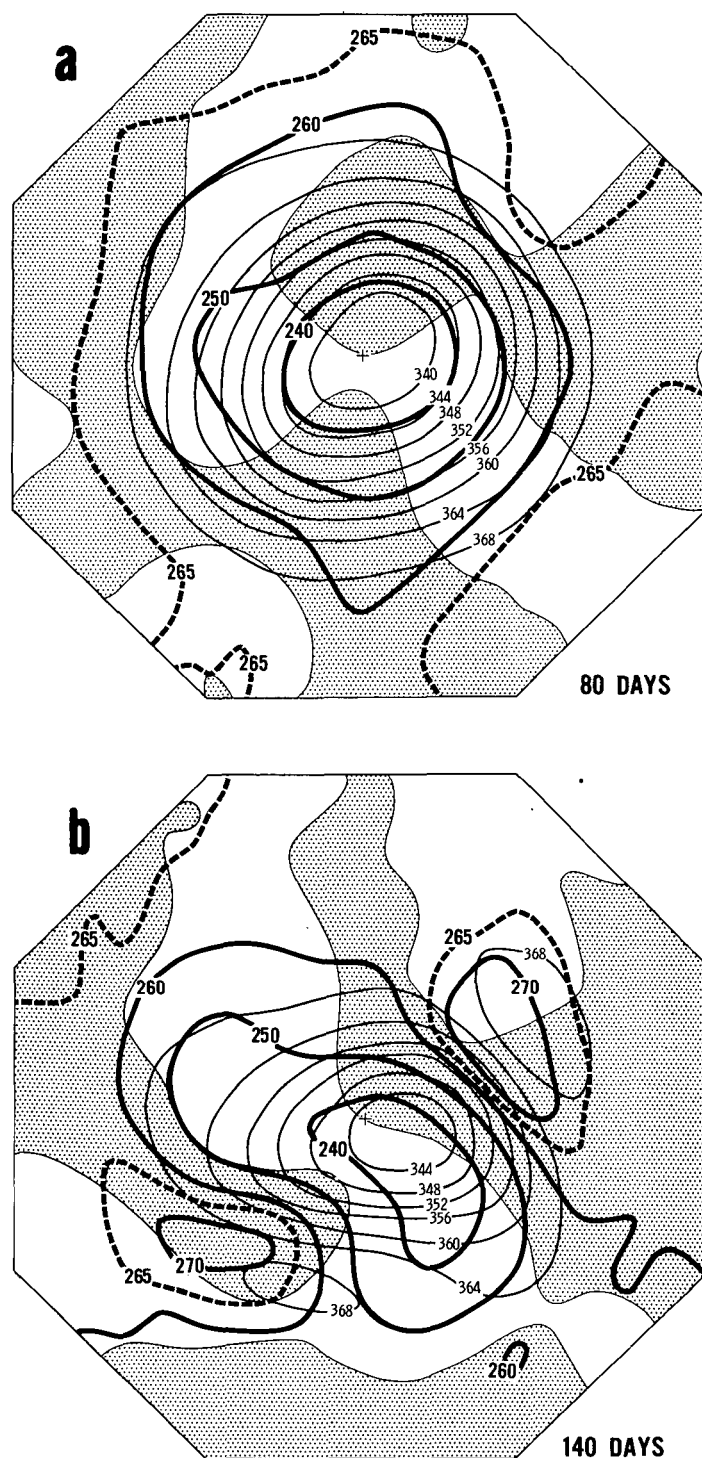


FIGURE 26.—The hemispheric variation of temperature (thick isolines), meridional velocity, and geopotential height (thin isolines) for the top level of the model at two different times illustrating the changes produced by the forcing from below. *S* areas are regions of northwards velocity. (Units: temperature, °K.; geopotential height, 100 m.)

by the eddies which the figure indicates can be expected at this time. This situation is very reminiscent of conditions in the actual stratosphere during the abnormal warming phenomenon of January 1957 described by Teweles [41]. The onset of the amplification of the wave in the top level was quite dramatic, and was first noticed in the time variation of the hemispheric integral of the

dissipation for that layer. Figure 27 shows that around 114 days a noticeable change must have occurred in the flow because of the rapid increase in the dissipation. A second, even larger growth in the dissipation occurred at about 138 days and was followed by a sudden decline to more normal values. The lower levels also experienced the same phenomenon but to a much lesser degree, and they also seem to have been affected at a slightly earlier time.

If the effects shown in figure 27 are attributable to a sudden onset of baroclinic instability, then it would be expected that the $-\overline{\omega'\alpha'}$ term for these levels would show a corresponding increase in order to maintain the kinetic energy against the rise in dissipation, as well as to supply energy for the development of the flow pattern. Although figure 28 reveals there was some increase in the release of potential energy during this period, the corresponding change in the eddy pressure interaction term leaves no doubt that it is the supply of energy from the lower levels that is responsible for the observed perturbations. The growth in this energy supply occurred at the same time as the dissipation increased on both occasions, and for the top level about 6 times as much energy came from below as was created *in situ*. This suggests that the increase in the conversion term at these times was caused by the changes produced in the flow patterns by forcing from below, rather than being examples of genuine baroclinic development. On a latitudinal basis most of supply of energy from below was confined between 45° and 70° lat., and this indicates that eddy kinetic energy was being given to the upper level jet, a result which might have been predicted from figure 21b. The consequent increase in the eddy kinetic energy in the top three levels of the model is illustrated in figure 29, and it is clear that it is closely related to the upwards flux of energy in figure 28. Part of this eddy kinetic energy was converted to zonal kinetic energy by the horizontal wind components. However, the energy flux from below is significantly larger than this conversion. The reason for the sudden increase in the energy transfer from below is unknown, but it might be indicative of the kind of interaction which takes place in the middle stratosphere prior to a stratospheric warming (see for example Miyakoda [24]). In this regard it is interesting to note that subsequent to the decline of the second impulse, the flow field in level 1 gradually returned to a more zonally symmetric state similar to that given in figure 26a. The possibility therefore exists that the first successful numerical simulation of a stratospheric abnormal warming may have occurred in the present model, albeit accidentally.

Because of the importance of the eddy pressure interaction component in the long-term maintenance of the winter stratosphere, as indicated in figure 24, and the relative smallness of the eddy conversion term, it appears that genuine baroclinic instability should not be expected in the middle stratosphere. In fact if the results of Lindzen [15] are valid at 30 km., then for a typical winter wind shear of $1.5\text{--}2.0$ m./sec. $^{-1}$ km. $^{-1}$, which exists at this altitude in the polar regions according to Batten [1], a growth rate of the order of 100 days for unstable waves

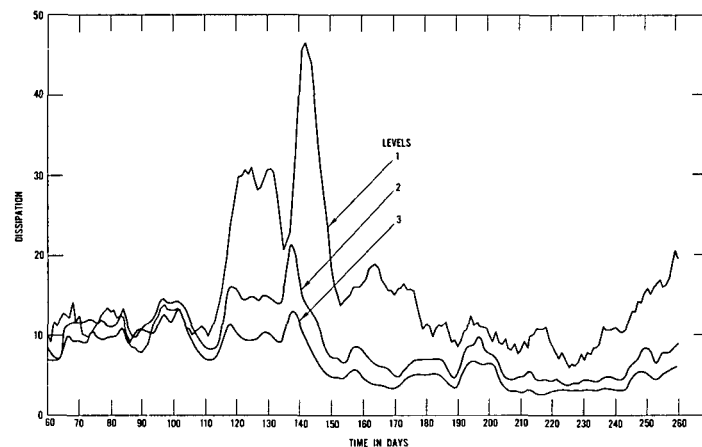


FIGURE 27.—The time variation of the hemispheric integral of dissipation for the top three levels of the model. (Units: 10^{-1} erg cm. $^{-2}$ mb. $^{-1}$ sec. $^{-1}$)

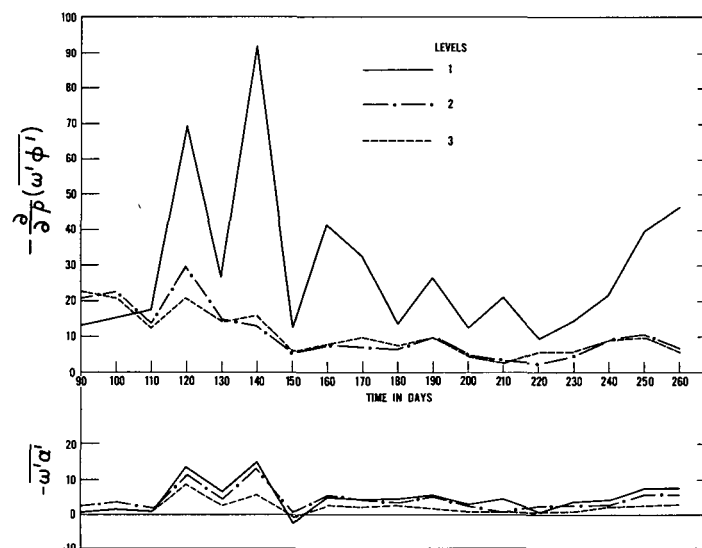


FIGURE 28.—The time variation of the eddy conversion of potential energy and the eddy pressure interaction term for the top three levels of the model. Values are based on 10-day time averages. (Units: 10^{-1} erg cm. $^{-2}$ mb. $^{-1}$ sec. $^{-1}$)

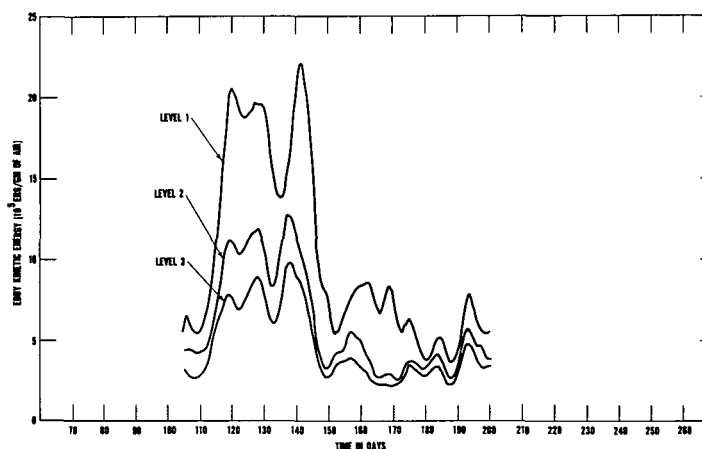


FIGURE 29.—The time variation of the hemispheric mean value of the eddy kinetic energy for the top three levels of the model. (Units: 10^5 ergs/gm.)

would be obtained. If allowance is also made for the seasonal variation it would seem that this growth rate is too slow to be effective. However, it does agree approxi-

mately with the time scale involved in the development of disturbances in the top layer of the model.

8. CONCLUDING REMARKS

The significant differences in the results of the present model compared with the 9-level model, which were produced by the doubling of the vertical resolution, particularly the remarkable improvement in the thermal structure of the stratosphere, would seem well worth the approximate doubling of the computation time involved. Although the results of the model are somewhat marred by the equatorwards shift of the atmospheric structure, it is hoped that this would only affect the results presented here and in Part II [7] quantitatively and not qualitatively. The intensity of the direct meridional cell in the Tropics is probably stronger than that in the atmosphere, and, while this may result in somewhat lower temperatures in the model than the atmosphere at the equatorial tropopause, it seems unlikely that this would alter the conclusions that the low temperatures and sharpness of the tropopause there, and also the height of the tropopause at low latitudes, are determined by the upwards motions associated with this cell. The present model should also clarify considerably the relative roles of radiation and dynamics in maintaining the midlatitude temperature maximum, as well as the relatively warm temperature at higher latitudes in the lower stratosphere. Contrary to some proposals that these regions are radiatively maintained, it was shown that radiation is actually trying to destroy them. The required heat is actually supplied by adiabatic warming associated with the downward branches of the meridional cells, and subsequent countergradient transport by the horizontal eddies. The significant Equator to Pole temperature difference at about the height of the tropical tropopause is one of the most satisfactory features of this model.

As regards the dynamic part of the model, the increased vertical resolution produced two distinct jet streams, as observed in the winter atmosphere, although the maximum wind intensities calculated were rather high. The improved resolution around the tropopause enhanced the agreement with observation of the energy balance of the lower stratosphere and confirmed previous work indicating that this region is forced by the troposphere. In this model the kinetic energy of stratospheric eddies was found to be supplied mainly through the eddy pressure interaction term, although there was also a contribution from the mean meridional term. The model also gave the previously unsuspected result that in winter the middle stratosphere, 4–23.4 mb., also receives energy from below via the eddy pressure interaction term, and that this was the largest single term in the energy balance of this region. In view of this, and despite the fact that the flow there is potential energy releasing, it seems unlikely that genuine baroclinic instability exists in this region. Most of the energy supplied to the middle stratosphere is used to maintain the upper level jet stream, although transport of energy from midlatitudes by the horizontal eddies is also required for this purpose.

During the period of the integration of the model, the rapid elongation of flow pattern took place in the middle stratosphere particularly around the 4-mb. level due mainly to the convergence of energy flux from below. The temperature pattern of the wave reminds us of the distribution which appears during the period of typical abnormal warming.

The 2-cell meridional structure of the stratosphere was of fundamental importance in maintaining the thermal and dynamic properties of this region.

The present model in its representation of the atmosphere has deteriorated in some aspects compared with the 9-level model. Thus the tropospheric jet is too far south and too intense, and a considerable part of the angular momentum of this jet is supplied from the high-latitude regions, in contrast with both the atmosphere and the previous model. In addition the west winds in the tropical troposphere have intensified, as have the equatorial meridional winds in the upper troposphere, neither of these features being observed in the actual atmosphere.

Finally, since the atmosphere differs from the model in having diurnal and seasonal changes, transport of latent heat, mountains, land-sea contrast, to name but a few of the differences, there is obviously much room for improvement. In view of these omissions it is necessary to accept the results of model calculations with some caution, as it is always possible that the right results may have been obtained for the wrong reasons. More physically realistic models currently under development at this Laboratory should be able to clarify the importance of the omissions from the present model some time in the future.

REFERENCES

1. E. S. Batten, "Wind Systems in the Mesosphere and Lower Ionosphere," *Journal of Meteorology*, vol. 18, No. 3, June 1961, pp. 283–291.
2. E. S. Batten, "A Model of the Seasonal and Latitudinal Variation of Zonal Winds and Temperatures in the Stratosphere Above 30 Km.," *Rand Corporation Memorandum RM-4144-PR*, 1964, 28 pp.
3. J. G. Charney, "The Dynamics of Long Waves in a Baroclinic Westerly Current," *Journal of Meteorology*, vol. 4, No. 5, Oct. 1947, pp. 135–162.
4. G. M. B. Dobson, A. W. Brewer, and B. M. Cwilog, "Meteorology of the Lower Stratosphere," *Proceedings of the Royal Society of London*, Ser. A, vol. 185, No. 1001, Feb. 1946, pp. 144–175.
5. R. M. Goody, "The Thermal Equilibrium at the Tropopause and the Temperature of the Lower Stratosphere," *Proceedings of the Royal Society of London*, Ser. A, vol. 197, 1949, pp. 487–505.
6. W. S. Hering and T. R. Borden, Jr., "Ozonesonde Observations Over North America," *U.S. Air Force, Cambridge Research Laboratories, Hanscom Field, Mass., Environmental Research Papers No. 38*, vol. 2, July 1934, 280 pp.
7. B. G. Hunt and S. Manabe, "Experiments With a Stratospheric General Circulation Model: II. Large-Scale Diffusion of Tracers in the Stratosphere," *Monthly Weather Review*, vol. 96, No. 8, Aug. 1968, pp. 503–539.
8. C. E. Jensen, "Energy Transformation and Vertical Flux Processes Over the Northern Hemisphere," *Journal of Geophysical Research*, vol. 66, No. 4, Apr. 1961, pp. 1145–1156.

9. A. Kasahara and W. M. Washington, "NCAR Global General Circulation Model of the Atmosphere," *Monthly Weather Review*, vol. 95, No. 7, July 1967, pp. 389-402.
10. J. S. Kennedy, "Energy Generation Through Radiative Processes in the Lower Stratosphere," *Massachusetts Institute of Technology, Planetary Circulations Project, Report No. 11*, 1964, 116 pp.
11. A. Kochanski, "Cross Sections of the Mean Zonal Flow and Temperature Along 80°W.," *Journal of Meteorology*, vol. 12, No. 2, Apr. 1955, pp. 95-106.
12. H. L. Kuo, "The Stability Properties and Structure of Disturbances in a Baroclinic Atmosphere," *Journal of Meteorology*, vol. 10, No. 4, Aug. 1953, pp. 235-243.
13. Y. Kurihara and J. L. Holloway, "Numerical Integration of a Nine-Level Global Primitive Equations Model Formulated by the Box Method," *Monthly Weather Review*, vol. 95, No. 8, Aug. 1967, pp. 509-530.
14. C. E. Leith, "Numerical Simulation of the Earth's Atmosphere," *Methods in Computational Physics*, Academic Press, New York, vol. 4, 1965, pp. 1-28.
15. R. S. Lindzen, "Radiative and Photochemical Processes in Mesospheric Dynamics: Part IV, Stability of a Zonal Vortex at Midlatitudes to Baroclinic Waves," *Journal of the Atmospheric Sciences*, vol. 23, No. 3, May 1966, pp. 350-359.
16. J. London, "A Study of the Atmospheric Heat Balance," *Final Report*, Contract AF19(122)-165, College of Engineering, New York University, 1957, 99 pp.
17. J. London, "The Distribution of Total Ozone Over the Northern Hemisphere," *Symposium on Atmospheric Ozone II, Arosa, IUGG, Monograph No. 19*, 1963, p. 46.
18. S. Manabe and F. Möller, "On the Radiative Equilibrium and Heat Balance of the Atmosphere," *Monthly Weather Review*, vol. 89, No. 12, Dec. 1961, pp. 503-532.
19. S. Manabe, J. Smagorinsky, and R. F. Strickler, "Simulated Climatology of a General Circulation Model With a Hydrologic Cycle," *Monthly Weather Review*, vol. 93, No. 12, Dec. 1965, pp. 769-798.
20. S. Manabe and R. F. Strickler, "Thermal Equilibrium of the Atmosphere With a Convective Adjustment," *Journal of the Atmospheric Sciences*, vol. 21, No. 4, July 1964, pp. 361-385.
21. H. J. Mastenbrook, "Water Vapor Observations at Low, Middle, and High Latitudes During 1964 and 1965," *Naval Research Laboratory Report 6447*, 1966, 199 pp.
22. Y. Mintz, "Very Long-Term Global Integration of the Primitive Equations of Atmospheric Motion," *World Meteorological Organization Technical Note No. 66*, Geneva, 1965, pp. 141-167.
23. Y. Mintz and J. Lang, "A Model of the Mean Meridional Circulation," *Final Report*, Contract AF19(122)-48, General Circulation Project, University of California at Los Angeles, Article 6; Mar. 1955, 10 pp.
24. K. Miyakoda, "Some Characteristic Features of Winter Circulation in the Troposphere and Lower Stratosphere," *Technical Report No. 14*, Science Foundation (Grant NSF-GP-471), Dept. of the Geophysical Sciences, University of Chicago, Dec. 1963, 93 pp.
25. H. S. Muench and T. R. Borden, Jr., "Atlas of Monthly Mean Stratosphere Charts, 1955-1959, Part II. July-December," *Air Force Surveys in Geophysics No. 141*, AFCRL-62-494[2], Air Force Cambridge Research Laboratories, Bedford, Mass., Oct. 1962.
26. F. W. Murray, "Dynamic Stability in the Stratosphere," *Journal of Geophysical Research*, vol. 65, No. 10, Oct. 1960, pp. 3273-3305.
27. R. E. Newell, "Stratospheric Energetics and Mass Transport," *Pure and Applied Geophysics*, Basel, Switzerland, vol. 58, No. II, 1964, pp. 145-156.
28. R. E. Newell, "The Energy and Momentum Balance of the Atmosphere Above the Tropopause," *Problems of Atmospheric Circulation*, edited by R. V. Garcia and T. F. Malone, Spartan Books, Washington, D.C., 1965, pp. 106-126.
29. G. O. P. Obasi, "Atmospheric Momentum and Energy Calculations for the Southern Hemisphere During the I.G.Y.," *Planetary Circulations Project Report No. 6*, Massachusetts Institute of Technology, 1963, 354 pp.
30. G. Ohring, "The Radiation Budget of the Stratosphere," *Scientific Report No. 1*, Contract AF19(604)-1738, Dept. of Meteorology and Oceanography, New York University, 1957, 42 pp.
31. A. H. Oort, "On the Energetics of the Mean and Eddy Circulations in the Lower Stratosphere," *Tellus*, vol. 16, No. 3, Aug. 1964, pp. 309-327.
32. E. Palmén and L. A. Vuorela, "On the Mean Meridional Circulations in the Northern Hemisphere During the Winter Season," *Quarterly Journal of the Royal Meteorological Society*, vol. 89, No. 379, Jan. 1963, pp. 131-138.
33. L. Peng, "A Modeling Study of the Meridional Temperature Profile and Energy Transformations in the Lower Stratosphere," *Planetary Circulations Project Report No. 13*, Massachusetts Institute of Technology, 1965, 161 pp.
34. N. A. Phillips, "The General Circulation of the Atmosphere: A Numerical Experiment," *Quarterly Journal of the Royal Meteorological Society*, vol. 82, No. 352, Apr. 1956, pp. 123-164.
35. C.-G. Rossby and R. B. Montgomery, "The Layer of Frictional Influence in Wind and Ocean Currents," *Papers in Physical Geography and Meteorology*, vol. 3, No. 3, Massachusetts Institute of Technology and Woods Hole Oceanographic Institution, 1935, 101 pp.
36. J. Smagorinsky, "General Circulation Experiments With the Primitive Equations: I. The Basic Experiment," *Monthly Weather Review*, vol. 91, No. 3, Mar. 1963, pp. 99-164.
37. J. Smagorinsky, S. Manabe, and J. L. Holloway, Jr., "Numerical Results From a Nine-Level General Circulation Model of the Atmosphere," *Monthly Weather Review*, vol. 93, No. 12, Dec. 1965, pp. 727-768.
38. V. Starr and R. M. White, "Balance Requirements of the General Circulation," *Studies of the Atmospheric General Circulation, Final Report, Part I*, Contract AF19(122)-153, Dept. of Meteorology, Massachusetts Institute of Technology, 1954, pp. 186-242.
39. V. P. Starr and J. M. Wallace, "Mechanics of Eddy Processes in the Tropical Troposphere," *Pure and Applied Geophysics*, Basel, Switzerland, vol. 58, No. II, 1964, pp. 138-144.
40. S. Teweles, "Spectral Aspects of the Stratospheric Circulation During the IGY," *Planetary Circulations Project Report No. 8*, Massachusetts Institute of Technology, 1963, 191 pp.
41. S. Teweles, "Anomalous Warming of the Stratosphere Over North America in Early 1957," *Monthly Weather Review*, vol. 86, No. 10, Oct. 1958, pp. 377-396.
42. J. M. Wallace, "Long Period Wind Fluctuations in the Tropical Stratosphere," *Planetary Circulations Project Report No. 19*, Massachusetts Institute of Technology, 1966, 167 pp.
43. R. M. White, "The Counter-Gradient Flux of Sensible Heat in the Lower Stratosphere," *Tellus*, vol. 6, No. 2, May 1954, pp. 177-179.
44. E. J. Williamson and J. T. Houghton, "Radiometric Measurements of Emission From Stratospheric Water Vapour," *Quarterly Journal of the Royal Meteorological Society*, vol. 91, No. 389, July 1965, pp. 330-338.
45. U.S. Air Force, *Handbook of Geophysics* (Revised Edition), The Macmillan Co., New York, 1960, 656 pp.